Theory of spin detection on the surface of diffusive topological insulators by means of ferromagnets: Establishing Onsager reciprocity and the importance of tunnel contact

Rik Dey,* Leonard F. Register, and Sanjay K. Banerjee
Microelectronics Research Center, University of Texas at Austin, Austin, Texas 78758, USA

(Received 4 June 2019; revised manuscript received 11 August 2019; published 12 September 2019)

A charge current on the surface of a topological insulator (TI) produces a surface spin polarization that can be measured experimentally using a ferromagnetic (FM) tunnel contact either in a three-terminal or a four-terminal potentiometric measurement. The potential measured on the FM contact depends on the direction and the magnitude of the surface charge current, as well as the FM magnetization direction relative to the spin polarization on the surface of the TI. In such a measurement, the resistance always obeys Onsager reciprocity, i.e., $R_{ab,cd}(+\vec{M}) = R_{cd,ab}(-\vec{M})$, where $R_{ab,cd}$ is the resistance measured with current injected between contacts a and b, voltage measured between contacts c and d, and the FM having magnetization $\vec{M}$. In a two-terminal measurement in which the current and the voltage contacts are the same, Onsager reciprocity dictates that the resistance remains the same even after the magnetization of the FM is reversed, i.e., $R_{ab,ab}(+\vec{M}) = R_{ab,ab}(-\vec{M})$. However, previous theories [Phys. Rev. Lett. **105**, 066802 (2010), Europhys. Lett. **93**, 67004 (2011)] claimed that change of resistance in such two-terminal measurement on the surface of a diffusive TI is possible upon reversing the FM magnetization direction. Here, we resolve this conflicting issue by showing that the Onsager reciprocity relation remains valid even in a two-terminal measurement on the surface of a diffusive TI. We consider the modifications in both the continuity equation of the charge density and the charge current density on the surface of the TI due to the effect of tunneling of electrons from the FM tunnel contact. We derive the transport equations on the surface of the TI from full quantum mechanical kinetic equation based on Keldysh Green's function, and obtain the resistance measured in a two-terminal or a multiterminal measurement after solving the transport equations analytically. We establish the validity of the Onsager reciprocity relation in both the two-terminal and the multiterminal measurements and also show the crucial importance of the tunnel contact in such spin detection experiments.

DOI: 10.1103/PhysRevB.100.094419

I. INTRODUCTION

Topological insulators (TIs) have gained considerable attention in spintronics research due to the nontrivial band structure of the gapless surface states with spin-momentum helical locking [1]. The spin-momentum locking in the two-dimensional (2D) surface states of a three-dimensional (3D) TI leads to a nonzero spin polarization within the surface states when charge current flows on the surface of the TI. This spin polarization can be detected experimentally using potentiometric multiterminal measurement set-ups including ferromagnetic metal (FM) tunnel contacts [2–14]. The voltage detected at the FM contact depends on the magnitude of the surface charge current and the angle between charge current-induced spin polarization on the surface of the TI and the magnetization direction of the FM [7,15–19]. The potentiometric measurement opens up the possibility of reading the FM magnetization in TI-FM-based memory and logic devices in which the FM bit is written by the charge current-induced spin polarization on the TI surface [20,21].

Spin detection experiments on the surface of a 3D TI using FM tunnel contacts have been performed in four-terminal [2–12] and three-terminal [13,14] potentiometric set-ups in which the FM tunnel contact can be used as a voltage probe or as a current probe. The measurement geometries are shown in Fig. 1. The multicontact resistance $R_{ab,cd}(\vec{M}) = V_{cd}/I_{ab}$ is recorded in the experiments, where V_{cd} is the voltage drop measured from contact c to contact d, and I_{ab} is the current applied from contact a to contact b, and $\vec{M}$ is the magnetization of the FM contact. The property of the spin-momentum locking of the surface states of a TI results in $R_{ab,cd}(+\vec{M}) \neq R_{ab,cd}(-\vec{M})$ and a variation of the multicontact resistance with the FM magnetization [2–14]. However, in a multiterminal measurement, $R_{ab,cd}(+\vec{M}) \neq R_{ab,cd}(-\vec{M})$ does not violate the Onsager reciprocity relation which says only that $R_{ab,cd}(+\vec{M}) = R_{cd,ab}(-\vec{M})$, where the voltage and the current contacts are interchanged along with the reversal of the magnetization direction [22].

In the case of a two-terminal measurement with a FM and a nonmagnetic metal (NM) contact shown in Fig. 2(a), the Onsager reciprocity relation $R_{ab,ab}(+\vec{M}) = R_{ab,ab}(-\vec{M})$ dictates that the two-terminal resistance will remain unchanged even if the magnetization of the FM is reversed, since the contact pair ab and cd are one and the same. Similarly, in case of a two-terminal measurement with two FM contacts, as shown in Fig. 2(b), the Onsager reciprocity relation requires that $R_{ab,ab}(\vec{M}_1, \vec{M}_2) = R_{ab,ab}(-\vec{M}_1, -\vec{M}_2)$, i.e., the resistance will remain the same if the magnetizations of both the FMs, $\vec{M}_1, \vec{M}_2$, are reversed. However, in the literature, it had been posited theoretically that two-terminal resistance between a

*Corresponding author: rikdey@utexas.edu

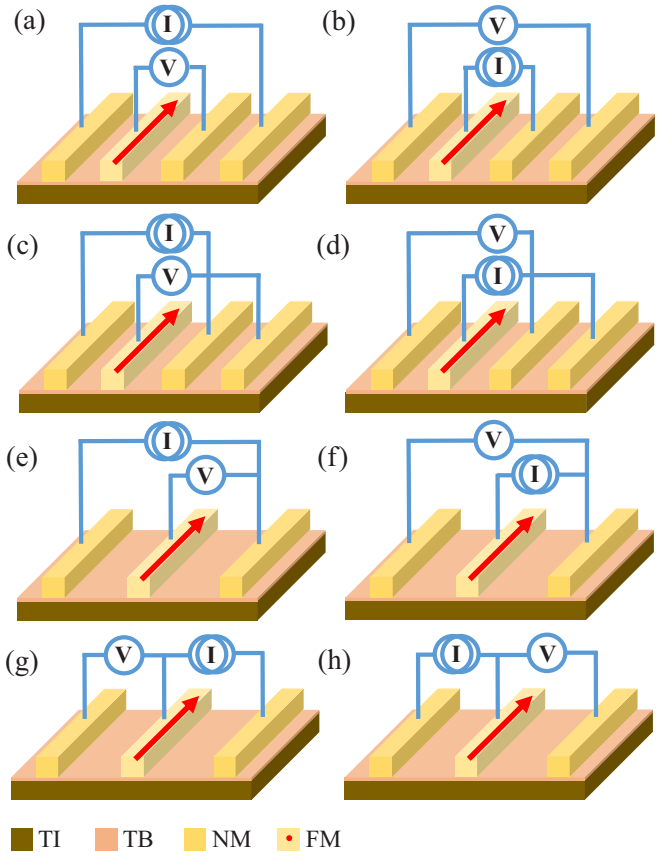

FIG. 1. Schematics of (a)–(d) four-terminal and (e)–(h) three-terminal spin-detection experiments on the surface of a diffusive TI.

FM and a NM contact or between two FM contacts on the surface of a TI can change depending on the magnetization of the FM, where the transport on the TI surface was assumed either purely diffusive [23–26], or purely ballistic [27], or partly diffusive and partly ballistic [28]. Such violations of Onsager reciprocity for two-terminal resistance also had been found experimentally on the surface of TIs [26,29–31].

In this paper, we derive the transport equations on the surface of a diffusive TI coupled to a FM tunnel contact, and then solve the resulting differential equations to obtain the resistances measured in such spin-detection experiments for four-terminal and three-terminal measurement geometries to demonstrate the validity of the Onsager reciprocity relation. Furthermore, we demonstrate the validity of the Onsager reciprocity relation for the two-terminal resistance between a FM and a NM contact or between two FM contacts, showing that the measured resistance is independent of reversal of the magnetization of the FM in the former case, or one or both magnetizations of the two FMs in the latter case consistent with Onsager reciprocity [15,19,22]. The validity of Onsager reciprocity for two-terminal resistance on the surface of a diffusive TI, in turn, calls for a reinterpretation of the experimental results for TIs [26,29–31]. For the detection of the charge current-induced spin polarization on the surface of a TI with a FM in a multiterminal measurement, the requirement of a tunnel barrier (TB) was clearly demonstrated in experiments [2–14]. Here we also show the importance of the tunnel contact in such experiments. We find that the spin detection efficiency, or the difference of the measured voltage at the FM contact on reversing the magnetization of the FM, decreases with decreasing resistance of the FM tunnel contact.

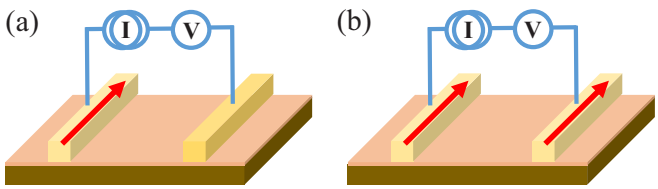

FIG. 2. Schematics of two-terminal measurements on the surface of a diffusive TI with (a) FM and NM contacts, (b) two FM contacts.

II. BACKGROUND AND MOTIVATION

We address possible one-dimensional (1D) circuit geometries that can be used to detect current-induced spin-polarization on the surface of a TI using four-terminal or three-terminal measurement set-ups. In a four-terminal setup, the FM contact can be used as a voltage probe to measure the charge current-induced spin polarization on the surface of the TI, as shown in Figs. 1(a) and 1(c). In these experiments, the current is passed through two NM contacts and the voltage is measured at the FM contact with respect to another NM contact different from the current injecting contacts. However, the reciprocal circuits, those obtained by flipping the voltage and current contacts of Figs. 1(a) and 1(c) are shown in Figs. 1(b) and 1(d), respectively, in which the FM contact will be a current probe, also can be used. In a three-terminal setup, the FM contact can be used as either a voltage probe with the voltage measured with respect to that on either one of the current injecting NM contacts, as shown in Fig. 1(e), or as a current probe, as shown in Fig. 1(f), which is the reciprocal circuit of Fig. 1(e), or as both voltage and current probes in which the current is passed through a FM and a NM contact and the voltage is measured between the same FM contact and another NM contact placed on other side of the current injecting NM contact, as shown in Figs. 1(g) and 1(h). The circuits shown in Figs. 1(g) and 1(h) are reciprocal circuits of each other. We show that the Onsager reciprocity relation is satisfied in each case by analyzing the reciprocal circuit pairs in the mentioned four-terminal and three-terminal measurement setups.

In the literature, Burkov *et al.* [23] and Schwab *et al.* [24] found theoretically that the two-terminal resistance measured on the surface (x-y plane) of a diffusive TI between a FM and a NM contact, as shown in Fig. 2(a), changes if the magnetization of the FM, which lies in the plane of the surface and normal (y axis) to the direction of transport (x axis), is reversed, which violates the Onsager reciprocity relation. In the theory of Burkov *et al.* [23], the coupled spin and charge diffusion equations on the surface of a TI were derived from density matrix response function formalism in a low-frequency long-wavelength limit, and the spin-charge coupled equations were solved analytically with current injected from a FM contact to the TI surface. However, in their work, the coupling of the FM contact to the TI surface states was not derived inside the theoretical framework, but,

rather, was inserted by hand as boundary conditions for the charge current density and the spin current density in the spin-charge coupled diffusion equation of the TI surface states. The resulting two-terminal resistance that was obtained from the solution of the coupled diffusion equations violates the Onsager reciprocity relation. Although, Schwab *et al.* [24] had considered the effect of coupling of the FM contact to the TI surface states through a tunneling self-energy in quantum mechanical Keldysh Green's function approach to derive a modified continuity equation of the charge density on the TI surface, the modification of the charge current density was not considered.

Following the approach by Burkov *et al.* [23], i.e., using the same spin-charge coupled diffusion equations on the TI surface and the same boundary conditions for the charge current density and the spin current density for the FM contact, Taguchi *et al.* [25] calculated the two-terminal resistance between two FM contacts on the surface of a diffusive TI, as shown in Fig. 2(b), and their results also violate the Onsager reciprocity relation. In a prior work [26], we found that the same spin-charge coupled diffusion equations on the surface of a TI without any tunneling from the FM also can be obtained in a different framework based on the quantum kinetic equation invoking the diffusive approximations used by Burkov *et al.* [23]. However, in all these previous works [23,25,26], the same boundary conditions were used to solve the same transport equations leading to the result of two-terminal resistances violating the Onsager reciprocity relation.

In this work, we show that the coupled diffusion equations on the surface of a TI are modified due to tunneling of electrons from a FM contact, and the actual effect of the FM contact cannot be taken into account simply by assuming charge current and spin current injection from the FM as boundary conditions. However, Schwab *et al.* [24] had only derived a modification of the continuity equation of the charge density due to tunneling while keeping the equation for charge current density unchanged; that is, in their work the charge current density was given by the gradient of the full nonequilibrium electrochemical potential—reexpressed in their work and this work as the effective nonequilibrium charge density—on the TI surface even after tunneling from the FM. Here we show that the charge current density on the TI surface also will contain an additional contribution due to tunneling from the FM, along with the gradient of the effective charge density term but with a modified diffusion constant or a modified conductivity. Considering both the modifications of the charge current density and the continuity equation of the charge density due to tunneling from the FM, we demonstrate that the two-terminal resistances between a FM and a NM contact or between two FM contacts on the surface of a diffusive TI satisfy the Onsager reciprocity relation. In case of two FM contacts, we show that the resistance remains the same whether the magnetizations of the two FMs are parallel or antiparallel, because the initial spin polarizations of the electrons that undergo tunneling from either of the FMs to the TI surface are lost after momentum scattering on the TI surface due to the spin-momentum locking of the TI surface states.

Finally, we also identify possible reasons behind the theoretical results obtained previously [23–26] leading to violation of Onsager reciprocity for the two-terminal resistance on the surface of a diffusive TI consisting of FM contacts. We show that the coupled spin-charge diffusion equations for the TI surface states obtained by Burkov *et al.* [23] do not satisfy the continuity equation of the charge density, where the charge current density is derived from the velocity operator obtained from the Hamiltonian of the TI surface states. However, Burkov *et al.* had defined both the charge current density and the spin current density on the TI surface from the coupled charge and spin transport equations considering continuity of the charge density and the spin density. We show that the definition of the charge current density obtained by them is inconsistent with the the charge current density obtained from the Hamiltonian of the TI surface states. Moreover, it was already discussed in the literature [32,33] that the definition of the spin current density obtained from the continuity equation for the spin density is not applicable for material with spin-momentum locked band structure. The physically measurable spin current density, which was used in the boundary condition for the spin current injection from the FM to the TI surface in prior works [23,25,26], was defined to be the gradient of the spin density on the TI surface. However, the spin current density being proportional to the gradient of the spin density on the TI surface is inconsistent with the formal definition of the spin current density derived from the TI surface state Hamiltonian [32,33]. In the work of Schwab *et al.* [24], the modification of the charge current density on the TI surface due to tunneling from the FM was not considered, which did lead to the violation of the Onsager reciprocity relation. Here we show that considering both the modifications of the charge current density and the continuity equation of the charge density, indeed, results in the two-terminal resistance that satisfies Onsager reciprocity.

III. THEORY

A. Derivation of the transport equations

The low-energy effective Hamiltonian of the TI surface states is given by $H(\mathbf{p}) = \hbar v_F(\mathbf{p} \times \hat{\mathbf{z}}) \cdot \boldsymbol{\sigma}$, where $\hbar$ is the reduced Planck constant, v_F is the Fermi velocity of the TI surface states, $\mathbf{p}$ is the 2D momentum of the surface states, $\hat{\mathbf{z}}$ is the unit vector along the surface normal direction, and $\boldsymbol{\sigma} = (\sigma_x, \sigma_y, \sigma_z)$ is the vector consisting of the Pauli spin matrices. We consider the transport within the TI surface in the TI-FM contact layer as shown in Fig. 4 below. The momentum scattering among the TI surface states is considered due to random spin-independent short-range impurity potentials on the surface of the TI consistent with both Schwab *et al.* [24] and Burkov *et al.* [23], neglecting phonon at the considered low temperatures in the experiments. In Schwab *et al.* [24], the coupling of the TI surface states to the FM contacts are modeled by spin-conserving but momentum-randomizing tunneling, where the work of Burkov *et al.* [23] did not directly model tunneling. In this work, we mainly focus on the spin-conserving momentum-randomizing tunneling between the FM and TI surface states to allow for a direct comparison to the work of Schwab *et al.* [24]. However, we also discuss the effect of spin-nonconserving but spin-selecting and momentum-randomizing or in-plane momentum-conserving tunneling on the spin-detection experiments. Both the effects

of tunneling from the FM to the TI surface states and the momentum scattering among the TI surface states are included in the quantum kinetic equation through self-energy contributions.

The quantum kinetic equation can be written in terms of the Green's function g of the TI surface states as (see Appendix A):

$$\begin{aligned}\partial_t \mathrm{g} + \frac{v_\mathrm{F}}{2}\{(\hat{\mathbf{z}}\times\boldsymbol{\sigma})\cdot\boldsymbol{\nabla}_\mathbf{R},\mathrm{g}\} + iv_\mathrm{F}\mathrm{p_F}[(\hat{\mathbf{p}}\times\hat{\mathbf{z}})\cdot\boldsymbol{\sigma},\mathrm{g}]\\ = -\frac{1}{\tau_\mathrm{p}}(\mathrm{g}-\langle\mathrm{g}\rangle) + \frac{1}{2\tau_\mathrm{p}}\{(\hat{\mathbf{p}}\times\hat{\mathbf{z}})\cdot\boldsymbol{\sigma},\langle\mathrm{g}\rangle\}\\ - \gamma(\{(N_\uparrow\mathrm{P}_\uparrow + N_\downarrow\mathrm{P}_\downarrow),\mathrm{g}\} + N_\uparrow\mathrm{P}_\uparrow\mathrm{g}_\uparrow + N_\downarrow\mathrm{P}_\downarrow\mathrm{g}_\downarrow)\\ + \frac{\gamma}{2}\{(\hat{\mathbf{p}}\times\hat{\mathbf{z}})\cdot\boldsymbol{\sigma},(N_\uparrow\mathrm{P}_\uparrow\mathrm{g}_\uparrow + N_\downarrow\mathrm{P}_\downarrow\mathrm{g}_\downarrow)\}. \qquad (1)\end{aligned}$$

In the above equation, the Green's function $\mathrm{g}(\mathbf{R},t;\mathrm{p_F}\hat{\mathbf{p}},\varepsilon)$ is expressed in terms of the Wigner coordinates $(\mathbf{R},t;\mathrm{p_F}\hat{\mathbf{p}},\varepsilon)$, where $\mathbf{R}$ is the position on the TI surface, t is time, $\mathrm{p_F}$ is the Fermi momentum magnitude of the TI surface states, $\hat{\mathbf{p}} = \mathbf{p}/\mathrm{p_F}$ is the unit vector, and ε is energy. In Eq. (1), τ_p is the scattering time between the Bloch states of the TI (τ_p would be the momentum relaxation time on the surface of the TI in the absence of consideration of the overlap of the initial and final states of the TI, where the second term on the second line of Eq. (1) then address this spin overlap between initial and final states of the TI), γ denotes the strength of tunneling between the FM and the TI surface states, $\langle\cdot\rangle$ denotes angular averaging over the Fermi contour of the TI surface states, $\mathrm{P}_{\uparrow,\downarrow} = (\sigma_0 \pm \hat{\mathbf{m}}\cdot\boldsymbol{\sigma})/2$ are the projection operators to the majority and minority spin bands in the FM, σ_0 is the spin-space identity matrix, $\hat{\mathbf{m}} = (m_x, m_y, m_z)$ is the magnetization direction (a unit vector) of the FM, $N_{\uparrow,\downarrow}$ are the corresponding density of states (DOSs) of the majority and minority spin bands in the FM at the Fermi energy, and $\mathrm{g}_{\uparrow,\downarrow}$ are the nonequilibrium quasiclassical Green's functions of the majority and minority electrons in the FM averaged over the Fermi surface in the FM.

The derivation of Eq. (1) is given in detail in Appendix A following our previous work [34]. However, in our previous work, to obtain the continuity equation of the charge density and the charge current density on the TI surface, we solved the quasiclassical Green's function g of the TI surface states assuming projection of g on the conduction band of the Hamiltonian, i.e., $\mathrm{g} = \mathrm{g}_0(\hat{\mathbf{p}},\varepsilon)[\sigma_0 + (\hat{\mathbf{p}}\times\hat{\mathbf{z}})\cdot\boldsymbol{\sigma}]$, and expanding the angular dependence of g in the zeroth and the first harmonics, i.e., $\mathrm{g}_0(\hat{\mathbf{p}},\varepsilon) = \mathrm{g_s}(\varepsilon) + \hat{\mathbf{p}}\cdot\mathbf{g}_\mathrm{a}(\varepsilon)$. In this work, we proceed differently to derive the transport equations on the TI surface, with one aim of this approach being to connect the work of Burkov *et al.* [23] and that of Schwab *et al.* [24]. In our approach, on one hand, the spin-charge coupled diffusion equations given by Burkov *et al.* [23] can be derived in the absence of tunneling [26], and it can be shown easily that the spin-charge coupled diffusion equations given by Burkov *et al.* [23] violates the continuity equation of the charge density on the TI surface, where the charge current density on the TI surface is defined using the velocity operator for the surface states $\mathbf{v} = (1/\hbar)\partial H/\partial\mathbf{p} = v_\mathrm{F}(\hat{\mathbf{z}}\times\boldsymbol{\sigma})$. On the other hand, for the tunneling of carriers between the FM and the TI surface, the modification of the continuity equation of the charge density on the TI surface given by Schwab *et al.* [24] can be obtained, along with a modification of the charge current density that was not considered by Schwab *et al.* [24], but that cannot be disregarded in the transport on the surface of a diffusive TI coupled to a FM.

The quasiclassical Green's function g of the TI surface states can be written as $\mathrm{g} = \mathrm{g}_0\sigma_0 + \mathbf{g}\cdot\boldsymbol{\sigma}$, where $\mathbf{g} = (\mathrm{g}_x, \mathrm{g}_y, \mathrm{g}_z)$. By Fourier transforming $\partial_t \to -i\omega$ and $\boldsymbol{\nabla}_\mathbf{R} \to i\mathbf{q} = (i\mathrm{q}_x, i\mathrm{q}_y)$, and taking trace of Eq. (1) after multiplying by identity matrix and each of three Pauli spin matrices, the resulting four equations can be rewritten in matrix form as

$$\mathbb{K}g = \mathbb{L}(\langle g\rangle + h), \qquad (2)$$

where $g = (\mathrm{g}_0, \mathrm{g}_x, \mathrm{g}_y, \mathrm{g}_z)^T$ and $h = (\mathrm{h}_0, \mathrm{h}_x, \mathrm{h}_y, \mathrm{h}_z)^T$ are 4×1 column vectors, $\mathbb{K}$ and $\mathbb{L}$ are 4×4 matrices. Here $\mathrm{h}_0 = \gamma\tau_\mathrm{p}(N_\uparrow\mathrm{g}_\uparrow + N_\downarrow\mathrm{g}_\downarrow)/2$ and $(\mathrm{h}_x, \mathrm{h}_y, \mathrm{h}_z) = \mathbf{h}$ is given by $\mathbf{h} = \gamma\tau_\mathrm{p}(N_\uparrow\mathrm{g}_\uparrow - N_\downarrow\mathrm{g}_\downarrow)\mathbf{m}/2$. The matrix $\mathbb{L}$ is given by

$$\mathbb{L} = \begin{bmatrix} 1 & \sin\theta & -\cos\theta & 0\\ \sin\theta & 1 & 0 & 0\\ -\cos\theta & 0 & 1 & 0\\ 0 & 0 & 0 & 1\end{bmatrix}, \qquad (3)$$

where θ is the angle of the $\mathbf{p}$ vector lying on the Fermi contour. The matrix $\mathbb{K}$ is given by

$$\mathbb{K} = \begin{bmatrix} \Omega & i\Delta_y & -i\Delta_x & \Delta_z\\ i\Delta_y & \Omega & 0 & \Omega_{SO}\cos\theta\\ -i\Delta_x & 0 & \Omega & \Omega_{SO}\sin\theta\\ \Delta_z & -\Omega_{SO}\cos\theta & -\Omega_{SO}\sin\theta & \Omega\end{bmatrix}, \qquad (4)$$

where $\Omega = 1 + \gamma N_+\tau_\mathrm{p} - i\omega\tau_\mathrm{p}$, $\Omega_{SO} = 2\mathrm{p_F}v_\mathrm{F}\tau_\mathrm{p}$, $\Delta_x = \mathrm{q}_x v_\mathrm{F}\tau_\mathrm{p} + i\gamma N_-\tau_\mathrm{p}m_y$, $\Delta_y = \mathrm{q}_y v_\mathrm{F}\tau_\mathrm{p} - i\gamma N_-\tau_\mathrm{p}m_x$, $\Delta_z = \gamma N_-\tau_\mathrm{p}m_z$, and $N_\pm = N_\uparrow \pm N_\downarrow$. The matrix $\mathbb{K}$ of Eq. (4) reduces to the one obtained previously in deriving the diffusion equation on the surface of a TI without a FM [26,35] after substituting $\gamma = 0$ in the quantities Ω, Δ_x, Δ_y, and Δ_z.

To obtain the diffusion equation, one has to solve for $\langle g\rangle$ in Eq. (2). Multiplying by $\mathbb{K}^{-1}$ on both sides of Eq. (2) and averaging over θ, $\langle g\rangle$ is obtained from the matrix equation

$$\langle g\rangle = \mathbb{D}(\langle g\rangle + h), \qquad (5)$$

where $\mathbb{D} = \langle\mathbb{K}^{-1}\mathbb{L}\rangle$ is a 4×4 matrix. Equation (5) is the most general form of spin-charge coupled transport equation on the surface of a TI coupled to a FM. However, in our case, the calculation of the matrix elements of $\mathbb{D}$ can be further simplified. As shown in Figs. 1 and 2, we only consider 1D problems with the FM magnetized in the $\pm y$ direction. Therefore, the charge and spin density will be uniform along the y direction on the TI surface. Hence, $\mathrm{q}_y = 0$ and $\mathbf{m} = (0, \pm 1, 0)$, therefore,

$\Delta_y = \Delta_z = 0$, and $\mathbb{K}^{-1}$ becomes [26,35]

$$\mathbb{K}^{-1} = \frac{\begin{bmatrix} \Omega(\Omega^2+\Omega_{SO}^2) & -i\sin\theta\cos\theta\Delta_x\Omega_{SO}^2 & i\Delta_x(\Omega^2+\Omega_{SO}^2\cos^2\theta) & -i\sin\theta\Delta_x\Omega\Omega_{SO} \\ -i\sin\theta\cos\theta\Delta_x\Omega_{SO}^2 & \Omega(\Omega^2+\Omega_{SO}^2\sin^2\theta+\Delta_x^2) & -\sin\theta\cos\theta\Omega\Omega_{SO}^2 & -\cos\theta(\Omega^2+\Delta_x^2)\Omega_{SO} \\ i\Delta_x(\Omega^2+\Omega_{SO}^2\cos^2\theta) & -\sin\theta\cos\theta\Omega\Omega_{SO}^2 & \Omega(\Omega^2+\Omega_{SO}^2\cos^2\theta) & -\sin\theta\Omega^2\Omega_{SO} \\ i\sin\theta\Delta_x\Omega\Omega_{SO} & \cos\theta(\Omega^2+\Delta_x^2)\Omega_{SO} & \sin\theta\Omega^2\Omega_{SO} & \Omega(\Omega^2+\Delta_x^2) \end{bmatrix}}{\Omega^2(\Omega^2+\Omega_{SO}^2)+\Delta_x^2(\Omega^2+\Omega_{SO}^2\cos^2\theta)}. \quad (6)$$

The form of the matrix $\mathbb{K}^{-1}$ given in Eq. (6) is the same as that obtained previously for the transport of the TI surface states without a FM [26,35], the only difference is the modification of the quantities Ω and Δ_x due to tunneling from the FM. To obtain $\mathbb{D}$, we need to integrate over angle θ, while the quantities Ω_{SO}, Ω and Δ_x are constants. Hence, some of the prior results for calculating the matrix elements of $\mathbb{D}$ can be straightforwardly reused. Mainly, after averaging $\mathbb{K}^{-1}\mathbb{L}$ over θ, the nondiagonal terms of the matrix $\mathbb{D}$ relating coupled transport of the g_0, g_y components with the g_x, g_z components vanish. That is, $\mathbb{D}_{0x}$, $\mathbb{D}_{x0}$, $\mathbb{D}_{0z}$, $\mathbb{D}_{z0}$, $\mathbb{D}_{xy}$, $\mathbb{D}_{yx}$, $\mathbb{D}_{yz}$, $\mathbb{D}_{zy}$ are zero since $\int_0^{2\pi} d\theta \sin\theta F(\cos\theta) = 0$ and $\int_0^{2\pi} d\theta \cos\theta F(\sin\theta) = 0$ for any smooth function F. Therefore, the spin in the x and z directions of the electrons are decoupled from the charge flow and y component of spin. However, the charge flow and the y component of spin of the electrons on the TI surface remain coupled. So we only work with the 2×2 matrix $\mathbb{D}_2$ consisting of $\mathbb{D}_{00}$, $\mathbb{D}_{0y}$, $\mathbb{D}_{y0}$, $\mathbb{D}_{yy}$ terms, and write the spin-charge coupled transport equation as

$$\langle g_2\rangle = \mathbb{D}_2(\langle g_2\rangle + h_2), \quad (7)$$

where $g_2 = (g_0, g_y)^T$ and $h_2 = (h_0, h_y)^T$ are 2×1 column vectors, and $\mathbb{D}_2$ is a 2×2 matrix given by

$$\mathbb{D}_2 = \begin{bmatrix} f_1 & \frac{i}{\Delta_x}(1-\Omega f_1) \\ \frac{i}{\Delta_x}(1-\Omega f_1) & \frac{\Omega}{\Delta_x^2}(1-\Omega f_1) \end{bmatrix}, \quad (8)$$

where

$$f_1 = \frac{\sqrt{\Omega^2+\Omega_{so}^2}}{\sqrt{\Omega^2+\Delta_x^2}\sqrt{\Omega^2+\Delta_x^2+\Omega_{so}^2}}. \quad (9)$$

B. Definitions of the effective charge densities and the full electrochemical potentials

The actual nonequilibrium component of the charge density of the electrons on the TI surface is denoted by $n_{\rm neq}$, which is the difference between the actual nonequilibrium charge density and the actual equilibrium charge density on the TI surface. Then $n_{\rm neq}$ is obtained from [24]

$$\begin{aligned} n_{\rm neq} &= \frac{eN}{2}\int \frac{1}{2}{\rm Tr}[\langle g(\varepsilon)\rangle]\, d\varepsilon - e^2N\phi \\ &= \frac{eN}{2}\int \langle g_0(\varepsilon)\rangle\, d\varepsilon - e^2N\phi, \end{aligned} \quad (10)$$

where N is the DOS of the TI surface states at the equilibrium Fermi energy and ϕ is the electrostatic potential on the TI surface resulting from any electric field. In this work, following the notation of Burkov *et al.* [23], the actual nonequilibrium component of the charge density $n_{\rm neq}$ and the external electrostatic potential ϕ are subsumed into the definition of the charge density for convenience; that is, on the surface of the TI, we define the effective nonequilibrium component of the charge density n as $n \equiv n_{\rm neq} + e^2N\phi$. Hence, by this definition, from Eq. (10) we have

$$n = \frac{eN}{2}\int \langle g_0(\varepsilon)\rangle\, d\varepsilon. \quad (11)$$

We define the electron-charge-normalized full nonequilibrium electrochemical potential μ on the TI surface by the relation $n \equiv e^2N\mu$. In this way, the effective nonequilibrium component of the charge density n and the full nonequilibrium electrochemical potential μ relative to the equilibrium value include variations in the Fermi level relative to the band edge and variations in the band edge with the electrostatic potential. So μ is given by

$$\mu = \frac{1}{2e}\int \langle g_0(\varepsilon)\rangle\, d\varepsilon. \quad (12)$$

It should be noted that the voltage difference on the TI surface will be just the difference of the electron-charge-normalized full nonequilibrium electrochemical potential μ, which is consistent with Burkov *et al.* [23].

The nonequilibrium spin density $\mathbf{s}$ (in the unit of electron charge) on the TI surface is given by [24]

$$\mathbf{s} = \frac{eN}{4}\int \frac{1}{2}{\rm Tr}[\langle \boldsymbol{\sigma} g(\varepsilon)\rangle]\, d\varepsilon = \frac{eN}{4}\int \langle \mathbf{g}(\varepsilon)\rangle\, d\varepsilon. \quad (13)$$

Here $\mathbf{s} = (s_x, s_y, s_z)$, and, s_x, s_y, s_z are the x, y, and z components of the spin density on the TI surface, respectively. The 2D charge current density $\mathbf{j}$ on the TI surface is given by [24]

$$\mathbf{j} = \frac{eN}{2}\int \frac{1}{2}{\rm Tr}[\langle \mathbf{v} g(\varepsilon)\rangle]\, d\varepsilon, \quad (14)$$

where $\mathbf{v} = v_{\rm F}(\hat{\mathbf{z}}\times\boldsymbol{\sigma})$ is the velocity operator. Here $\mathbf{j} = (j_x, j_y)$, and j_x and j_y are the x and y components of the 2D charge current density, respectively. Because of the spin-momentum locking of the TI surface states, the 2D charge current density $\mathbf{j}$ is related to the nonequilibrium spin density $\mathbf{s}$ by $\mathbf{j} = 2v_{\rm F}(\hat{\mathbf{z}}\times\mathbf{s})$. Hence, the charge current density j_x on the TI surface along the x direction is related to the y component of the spin density s_y on the TI surface by

$$j_x = -2v_{\rm F}s_y. \quad (15)$$

In the FM contact, the actual nonequilibrium components $n_{{\rm neq};\uparrow,\downarrow}$ of the charge densities of the majority and minority

spin electrons are obtained from, much as of Eq. (10),

$$n_{\mathrm{neq};\uparrow,\downarrow} = \tfrac{eN_{\uparrow,\downarrow}}{2}\int \tfrac{1}{2}\mathrm{Tr}[\mathrm{P}_{\uparrow,\downarrow}\mathrm{g}_{\uparrow,\downarrow}(\varepsilon)]\,d\varepsilon - e^2N_{\uparrow,\downarrow}\phi_{\mathrm{c}} = \tfrac{eN_{\uparrow,\downarrow}}{4}\int \mathrm{g}_{\uparrow,\downarrow}(\varepsilon)\,d\varepsilon - e^2N_{\uparrow,\downarrow}\phi_{\mathrm{c}}, \tag{16}$$

where ϕ_{c} is the electrostatic potential within the FM resulting from any electric field. We define the effective nonequilibrium components of the majority and minority electron charge densities $n_{\uparrow,\downarrow}$ by $n_{\uparrow,\downarrow} \equiv n_{\mathrm{neq};\uparrow,\downarrow} + e^2N_{\uparrow,\downarrow}\phi_{\mathrm{c}}$. Hence, by these definitions, from Eq. (16) we obtain

$$n_{\uparrow,\downarrow} = \frac{eN_{\uparrow,\downarrow}}{4}\int d\varepsilon\ \mathrm{g}_{\uparrow,\downarrow}(\varepsilon). \tag{17}$$

We define the electron-charge-normalized full nonequilibrium electrochemical potentials $\mu_{\uparrow,\downarrow}$ of the majority and minority spin electrons in the FM relating to the effective nonequilibrium components of the majority and minority electron charge densities $n_{\uparrow,\downarrow}$ by $n_{\uparrow,\downarrow} \equiv e^2N_{\uparrow,\downarrow}\mu_{\uparrow,\downarrow}$. So we have

$$\mu_{\uparrow,\downarrow} = \frac{1}{4e}\int d\varepsilon\ \mathrm{g}_{\uparrow,\downarrow}(\varepsilon). \tag{18}$$

The definitions of μ and $\mu_{\uparrow,\downarrow}$ match with those by Schwab *et al.* [24]. The meaning of electron-charge-normalized full nonequilibrium electrochemical potentials $\mu_{\uparrow,\downarrow}$ is up and down spin-voltages in the FM as mentioned by Schwab *et al.* [24].

IV. RESULTS AND DISCUSSIONS

A. Transport on TI surface and conservation of charge

To obtain the transport equations, we multiply both sides of Eq. (7) by $\mathbb{D}_2^{-1}$ to obtain the new matrix equation

$$\left[\mathbb{D}_2^{-1} - \mathbb{I}_2\right]\langle g_2\rangle = h_2, \tag{19}$$

where $\mathbb{D}_2^{-1}$ is given by

$$\mathbb{D}_2^{-1} = \begin{bmatrix} \Omega & -i\Delta_x \\ -i\Delta_x & f_2 \end{bmatrix} \tag{20}$$

and

$$f_2 = \frac{\Delta_x^2}{\Omega}\left(\frac{1}{f_1\Omega} - 1\right)^{-1}. \tag{21}$$

In the case of zero tunneling, $\gamma = 0$, hence, $h_2 = 0$, $\Omega = 1 - i\omega\tau_{\mathrm{p}}$ and $\Delta_x = \mathrm{q}_x v_{\mathrm{F}}\tau_{\mathrm{p}}$ in Eqs. (19), (20), and (21). After the ε integration of Eq. (19) and using Eq. (20), we obtain

$$\begin{bmatrix} \Omega - 1 & -i\Delta_x \\ -i\Delta_x & f_2 - 1 \end{bmatrix}\begin{bmatrix} n \\ 2s_y \end{bmatrix} = 0. \tag{22}$$

The first row of the matrix equation Eq. (22) gives

$$(\Omega - 1)n - 2i\Delta_x s_y = 0. \tag{23}$$

To obtain the second equation from the second row of the matrix equation Eq. (22), the function f_2 in Eq. (21) is approximated by series expansions in powers of Δ_x and Ω under the low-frequency, long-wavelength diffusive limit approximations, $\omega\tau_{\mathrm{p}} \ll 1$, $\mathrm{q}_x l_{\mathrm{p}} \ll 1$, and assuming that the Fermi energy lies well above the Dirac point, $\mathrm{p}_{\mathrm{F}} l_{\mathrm{p}} \gg 1$, where $l_{\mathrm{p}} = v_{\mathrm{F}}\tau_{\mathrm{p}}$ is the mean-free path on the TI surface. These approximations imply $|\Delta_x| \ll |\Omega| \ll 1 \ll \Omega_{\mathrm{so}}$; hence, f_2 can be approximated as $f_2 \approx 2\Omega$, i.e., $f_2 \approx 2 - 2i\omega\tau_{\mathrm{p}}$. Then, the second row of the matrix equation (22) gives

$$-i\Delta_x n + (2\Omega - 1)2s_y = 0. \tag{24}$$

Inverse Fourier transforming Eqs. (23) and (24), we obtain

$$\partial_t n - 2v_{\mathrm{F}}\partial_x s_y = 0, \tag{25a}$$

$$\partial_t s_y + \frac{s_y}{2\tau_{\mathrm{p}}} - \frac{v_{\mathrm{F}}}{4}\partial_x n = 0. \tag{25b}$$

Equations (25a) and (25b) describe the coupled nature of the charge and spin degrees of freedom of the TI surface states. From Eq. (25a), after using the relation between the charge current density j_x and the spin density s_y on the TI surface, i.e., $j_x = -2v_{\mathrm{F}}s_y$ as given in Eq. (15), we obtain the continuity equation of the charge density on the TI surface,

$$\partial_t n + \partial_x j_x = 0. \tag{26}$$

The continuity equation of the charge density, i.e., Eq. (26) is obtained from the first row of the matrix equation Eq. (22), and the continuity equation remains true irrespective of the approximation for the function f_2 that is used to derive Eq. (25b). Equation (25b) indicates that the spin relaxation time τ_{s} satisfies $\tau_{\mathrm{s}} = 2\tau_{\mathrm{p}}$, which is a property of the spin-momentum locked TI surface states [24,35]. In steady state, from Eq. (25b) we obtain $s_y = \frac{1}{2}v_{\mathrm{F}}\tau_{\mathrm{p}}\partial_x n$, and using $j_x = -2v_{\mathrm{F}}s_y$ [Eq. (15)], we obtain the charge current density on the TI surface,

$$j_x = -v_{\mathrm{F}}^2\tau_{\mathrm{p}}\partial_x n. \tag{27}$$

Equation (27) captures the charge current due to both drift and diffusion since the effective nonequilibrium component of the charge density n contains both the actual nonequilibrium component n_{neq} of the charge density of the electrons and any electrostatic field ϕ. Explicitly, after substituting $n = n_{\mathrm{neq}} + e^2N\phi$ in Eq. (27), we obtain $j_x = -D\partial_x n_{\mathrm{neq}} - \sigma\,\partial_x\phi$, where $D = v_{\mathrm{F}}^2\tau_{\mathrm{p}}$ is the diffusion constant on the TI surface and $\sigma = e^2ND$ is the associated conductivity via the Einstein relation for this degenerate system. It can be recognized that the diffusion constant $D = v_{\mathrm{F}}^2\tau_{\mathrm{p}} = v_{\mathrm{F}}^2\tau_{\mathrm{tr}}/2$, where we obtain the momentum relaxation time τ_{tr} to be $\tau_{\mathrm{tr}} = 2\tau_{\mathrm{p}}$ because of the spin-momentum locking of the TI surface states [24,34,36] (note that $\tau_{\mathrm{s}} = 2\tau_{\mathrm{p}} = \tau_{\mathrm{tr}}$). We refer to τ_{tr} as "the transport relaxation time" consistent with Schwab *et al.* [24]. In steady state, from Eqs. (26) and (27) we obtain

$$d_x j_x(x) = 0, \tag{28a}$$

$$j_x(x) = -\sigma d_x\mu(x), \tag{28b}$$

on the TI surface without any tunneling from the FM. Here and in what follows, we consider the full derivative d_x instead of the partial derivative ∂_x of preceding equations as we now have only an x dependence.

B. Modified transport on TI surface due to tunneling from FM

In the case of nonzero tunneling from the FM to the TI surface, we plug in $\Omega = 1 + \gamma N_+\tau_{\mathrm{p}} - i\omega\tau_{\mathrm{p}}$ and $\Delta_x = \mathrm{q}_x v_{\mathrm{F}}\tau_{\mathrm{p}} + i\gamma N_-\tau_{\mathrm{p}}m_y$ in Eqs. (20) and (21). After performing the ε integration of Eq. (19) and substituting Eq. (20), we

obtain

$$\begin{bmatrix} \Omega - 1 & -i\Delta_x \\ -i\Delta_x & f_2 - 1 \end{bmatrix} \begin{bmatrix} n \\ 2s_y \end{bmatrix} = \begin{bmatrix} \gamma N \tau_p n_+ \\ \gamma N \tau_p m_y n_- \end{bmatrix}, \tag{29}$$

where $n_\pm = n_\uparrow \pm n_\downarrow$. We define the dimensionless parameter $\xi = \gamma N_+ \tau_{tr} = 2\gamma N_+ \tau_p$, which is the normalized tunneling rate with respect to the momentum scattering rate on the TI surface, [36] and ξ is proportional to the tunnel conductance. In case of weak tunneling, $\xi \ll 1$, the conditions $|\Delta_x| \ll |\Omega| \ll 1 \ll \Omega_{so}$ remain valid, and f_2 given in Eq. (21) can be approximated as $f_2 \approx 2\Omega$, i.e., $f_2 \approx 2 + 2\gamma N_+ \tau_p - 2i\omega\tau_p$. After inverse Fourier transforming the first row of the matrix equation in Eq. (29) to real space, in steady state we obtain

$$d_x j_x = -\gamma N_+ n + \gamma N n_+ + \frac{\gamma N_- m_y}{v_F} j_x, \tag{30}$$

which is the modified continuity equation of the charge density on the TI surface due to tunneling from the FM to the TI. Similarly, after inverse Fourier transforming the second row of the matrix equation in Eq. (29) to real space and using $j_x = -2v_F s_y$, in steady state we obtain

$$j_x = \frac{1}{(1+\xi)}\big[- v_F^2 \tau_p \partial_x n + \gamma v_F \tau_p m_y (N_- n - N n_-)\big], \tag{31}$$

which is the diffusion equation for the current density on the surface of the TI including modifications due to tunneling from the FM to the TI. These two equations, Eqs. (30) and (31), are consistent with those we obtained in 2D transport in our previous work [34] and what was obtained from a semi-classical drift-diffusion model on the TI surface with tunneling calculated from the Golden Rule of scattering between the FM majority and minority electrons and the TI surface states [16].

Following the literature [16,24], we define the charge electrochemical potential μ_c in the FM as $\mu_c \equiv (\mu_\uparrow + \mu_\downarrow)/2$ and the spin electrochemical potential μ_s in the FM as $\mu_s \equiv (\mu_\uparrow - \mu_\downarrow)$. Under the charge neutrality condition in the FM contact, $n_{neq;\uparrow} + n_{neq;\downarrow} = 0$, and we obtain $\phi_c = \mu_c + \eta\mu_s/2$, where $\eta = N_-/N_+$ is the DOS polarization in the FM. In this work, following Schwab *et al.* [24], we assume $\mu_s = 0$, i.e., $\mu_\uparrow = \mu_\downarrow = \mu_c$, and we have $\mu_c = \phi_c$, which can be identified with the voltage in the FM [37]. Equation (30) then becomes

$$d_x j_x = \frac{2\xi\sigma}{l_{tr}^2}(\mu_c - \mu) + \frac{\xi\eta m_y}{l_{tr}} j_x, \tag{32}$$

and Eq. (31) becomes

$$j_x = -\frac{\sigma}{(1+\xi)}\left[d_x\mu + \frac{\xi\eta m_y}{l_{tr}}(\mu_c - \mu)\right], \tag{33}$$

where, $l_{tr} = v_F\tau_{tr} = 2v_F\tau_p$ is the transport relaxation length on the TI surface. The right-hand side of Eq. (32) can be interpreted as the current injected from the FM to the TI surface through the interface due to tunneling of electrons between the FM and the TI surface. The first term in the right hand side of Eq. (32) results from the difference of the electrochemical potential between the FM and the TI surface, and the tunnel conductance of the interface is proportional to $2\xi\sigma/l_{tr}^2$. The second term in the right-hand side of Eq. (32) results from the spin-momentum locking of the TI surface states and spin split bands of the FM. The first term in the right hand side of Eq. (33) is the diffusion term with the modified conductivity, $\sigma' = \sigma/(1+\xi)$, because tunneling back and forth across the interface serves as a momentum-randomizing scattering process for the TI surface states. The second term in the right hand side of Eq. (33) also arises because of the spin-momentum locking of the TI surface states and the spin split bands of the FM. The modification of the charge current density on the TI surface due to tunneling from the FM, given in Eq. (33), was not considered by Schwab *et al.* [24]. Although we have derived Eqs. (32) and (33) considering spin-conserving momentum-randomizing tunneling, the forms of (32) and (33) remain the same with a redefined ξ and η even if we consider spin-nonconserving but spin-selecting momentum-randomizing or in-plane momentum-conserving tunneling (see Appendix A). If the strength of tunneling between the TI surface states and the majority/minority bands of the FM are $\gamma_{\uparrow,\downarrow}$ which also depends on the nature of the interface (momentum randomization happens for a rough interface and in-plane momentum conservation holds for a smooth interface), then ξ and η should be redefined as $\xi = (\gamma_\uparrow N_\uparrow + \gamma_\downarrow N_\downarrow)\tau_{tr}$ and $\eta = (\gamma_\uparrow N_\uparrow - \gamma_\downarrow N_\downarrow)/(\gamma_\uparrow N_\uparrow + \gamma_\downarrow N_\downarrow)$.

C. Consideration of FM line contact

We begin our consideration of results for specific geometries by considering only line contacts in this section, which allows for more ready comparison to prior work by Schwab *et al.* [24]. In a subsequent section we extend our results to consider contacts of nonzero length. In deriving the two-terminal resistance between a FM and a point on the TI surface, Schwab *et al.* [24] had considered a FM line contact lying transverse to the transport direction and of infinitesimally small dimension along the transport direction, as shown in Fig. 3, with tunneling described by a δ function. We consider 1D transport along the x direction, the FM contact to be of length L along the transport direction located between region $x = 0$ and $x = L$ (we will take limit $L \to 0$) and of width W along the transport-normal direction y. The tunneling from the FM contact to the TI surface is modeled by replacing the tunneling strength γ by $\gamma L f_L(x)$, i.e., replacing ξ by $\xi L f_L(x)$, where $f_L(x)$ is a rectangular function with value $1/L$ in the region $x = 0$ to $x = L$ and zero otherwise. [Note that $f_L(x) \to \delta(x)$ in the limit $L \to 0$.] Following Schwab *et al.* [24], after replacing ξ by $\xi L f_L(x)$ we integrate Eq. (32) in a region $(-\epsilon, L+\epsilon)$ close to the FM contact, and let $\epsilon \to 0$ and $L \to 0$, to obtain

$$j_x^+ - j_x^- = \frac{2\xi\sigma L}{l_{tr}^2}\left(\mu_c^0 - \frac{\mu^+ + \mu^-}{2}\right) + \frac{\xi\eta m_y L}{l_{tr}}\frac{j_x^+ + j_x^-}{2}. \tag{34}$$

Here we denote μ_c^0 to be the electrochemical potential on the FM line contact, $\mu^+ = \mu(0^+)$ to be the electrochemical potential on the TI surface to the right of the FM line contact and $\mu^- = \mu(0^-)$ to be the electrochemical potential on the TI surface to the left of the FM line contact. Similarly, we denote $j_x^+ = j_x(0^+)$ to be the charge current density on the TI surface to the right of the FM line contact and $j_x^- = j_x(0^-)$ to be the charge current density on the TI surface to the left of the FM line contact. To obtain Eq. (34), we have used $\int_{-\epsilon}^{L+\epsilon} dx\, d_x j_x = j_x(L+\epsilon) - j_x(-\epsilon)$ and, in the

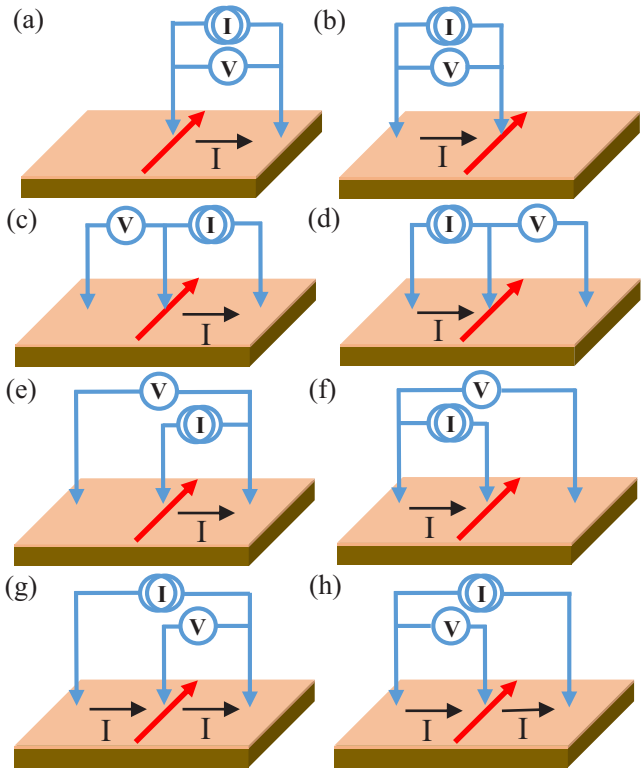

FIG. 3. Schematics of 1D measurement geometries on the surface of a diffusive TI with a line FM contact indicated by an arrow.

limits $\epsilon \to 0$ and $L \to 0$, $j_x(L+\epsilon) = j_x(0^+)$ and $j_x(-\epsilon) = j_x(0^-)$. Also in the limit $\epsilon \to 0$ and $L \to 0$, we have used $\int_{-\epsilon}^{L+\epsilon} dx f_L(x)\mu \approx \frac{1}{2}[\mu(0^+) + \mu(0^-)]$ and $\int_{-\epsilon}^{L+\epsilon} dx f_L(x) j_x \approx \frac{1}{2}[j_x(0^+) + j_x(0^-)]$ consistent with the approximations of Schwab *et al.* [24]. It should be noted that the electrochemical potential μ as well as the charge current density j_x on the TI surface will be continuous functions for $L \neq 0$, but the value of the function may be different to the right and left of the contact, i.e., $\mu(L^+) \neq \mu(0^-)$ and $j_x(L^+) \neq j_x(0^-)$ in general. In the limit $L \to 0$ for a line contact, there will be a change in the electrochemical potential on the TI surface across the FM line contact. This change in the electrochemical potential, which will be determined from Eqs. (32) and (33), was not considered by Schwab *et al.* [24].

Next, we consider Eq. (33), multiply both sides of Eq. (33) by $(1+\xi)$, replace ξ by $\xi L f_L(x)$, perform the integration of the resulting equation in a small region $(-\epsilon, L+\epsilon)$ with the limits $\epsilon \to 0$ and $L \to 0$, and divide the result by ξL, to obtain

$$\frac{j_x^+ + j_x^-}{2} = -\frac{\sigma}{\xi L}\left[(\mu^+ - \mu^-) + \frac{\xi \eta m_y L}{l_{\rm tr}}\left(\mu_{\rm c}^0 - \frac{\mu^+ + \mu^-}{2}\right)\right]. \tag{35}$$

To obtain Eq. (35), we have used $\int_{-\epsilon}^{L+\epsilon} dx\, d_x\mu = \mu(L+\epsilon) - \mu(-\epsilon)$, and, in the limits $\epsilon \to 0$ and $L \to 0$, $\mu(L+\epsilon) = \mu(0^+)$ and $\mu(-\epsilon) = \mu(0^-)$. Also, we have used $\int_{-\epsilon}^{L+\epsilon} dx\, j_x = 0$ in the limits $\epsilon \to 0$ and $L \to 0$. The electrochemical potential μ^+ and μ^- on the TI surface with respect to the electrochemical potential $\mu_{\rm c}^0$ on the FM will be determined in terms of the current density on the TI surface after solving Eqs. (34) and (35) with relevant boundary conditions on $j_x^{\pm}$.

In the measurement setups shown in Figs. 3(a), 3(c), and 3(e), a current I is injected from the FM contact to the TI surface to the right of the FM contact, so $j_x^+ = I/W$ and $j_x^- = 0$. Solving Eqs. (34) and (35), we obtain μ^+ and μ^- to be

$$\mu^+ = \mu_{\rm c}^0 - \left(1 - \frac{\eta^2 m_y^2}{2}\right)\frac{\xi I L}{4\sigma W} - \frac{l_{\rm tr}^2}{2\xi\sigma}\frac{I}{WL}, \tag{36a}$$

$$\mu^- = \mu_{\rm c}^0 + \left(1 - \frac{\eta^2 m_y^2}{2}\right)\frac{\xi I L}{4\sigma W} - \frac{l_{\rm tr}^2}{2\xi\sigma}\frac{I}{WL} + \frac{\eta m_y l_{\rm tr}}{2\sigma}\frac{I}{W}. \tag{36b}$$

The second term on the right side of both Eqs. (36a) and (36b) is the resistive potential drop due to the charge current flowing on the surface of the TI under the FM contact, where $\sigma W/L$ is the conductance of the TI surface over length L. The third term on the right side of both Eqs. (36a) and (36b) is the resistive potential drops across the interface due to the charge current flowing from the FM to the TI surface through the interface, where the interface conductance is $(2\xi\sigma/l_{\rm tr}^2)WL$, and WL is the area of the interface. [Note that $2\xi\sigma/l_{\rm tr}^2$ is the coefficient of the first term in Eq. (32).] From Eq. (36a), the potential drop $\Delta\mu(m_y) = (\mu_{\rm c}^0 - \mu^+)$ is indeed the same for $m_y = \pm 1$, and, hence, the two-terminal resistances measured between the FM and the TI surface, as shown in Fig. 3(a), is independent of the magnetization direction of the FM satisfying the Onsager reciprocity relation. However, the last term in μ^- is nontrivial due to the spin-momentum locking of the TI surface states. From Eq. (36b), the potential drop $\Delta\mu(m_y) = (\mu^- - \mu_{\rm c}^0)$, as shown in Fig. 3(c), depends on the sign of m_y. Similarly, from both Eqs. (36a) and (36b), the potential drop $\Delta\mu(m_y) = (\mu^- - \mu^+)$, as shown in Fig. 3(e), also depends on the sign of m_y. So the measured three-terminal resistances, as shown in Figs. 3(c) and 3(e), will depend on the magnetization direction of the FM. Such measurement setups were used to detect the current-induced spin polarization on the TI surface [13,14]. We define the spin-detection voltage $\delta\mu$ as the change of the potential drop upon reversing the magnetization direction of the FM, i.e., $\delta\mu = [\Delta\mu(m_y = +1) - \Delta\mu(m_y = -1)]$. In both cases shown in Figs. 3(c) and 3(d), $\delta\mu = \eta l_{\rm tr} I/\sigma W$.

In the measurement setups shown in Figs. 3(b), 3(d) and 3(f), a current I is extracted out of the FM contact from the TI surface to the left of the FM contact, such that $j_x^+ = 0$ and $j_x^- = I/W$. Then we obtain μ^+ and μ^- to be

$$\mu^+ = \mu_{\rm c}^0 - \left(1 - \frac{\eta^2 m_y^2}{2}\right)\frac{\xi I L}{4\sigma W} + \frac{l_{\rm tr}^2}{2\xi\sigma}\frac{I}{WL} + \frac{\eta m_y l_{\rm tr}}{2\sigma}\frac{I}{W}, \tag{37a}$$

$$\mu^- = \mu_{\rm c}^0 + \left(1 - \frac{\eta^2 m_y^2}{2}\right)\frac{\xi I L}{4\sigma W} + \frac{l_{\rm tr}^2}{2\xi\sigma}\frac{I}{WL}. \tag{37b}$$

The measurement setup pair shown in Figs. 3(a) and 3(b) [and, similarly, the pair Figs. 3(c) and 3(d) and the pair Figs. 3(e) and 3(f)] are identical after an 180° rotation in the plane. Hence, the solution for the electrochemical potential on the TI surface given in Eqs. (37a) and (37b) are related to that given in Eqs. (36a) and (36b), after a change of sign of both

I and m_y and the interchange of μ^+ and μ^-. The 180° rotation symmetry is also present in Eqs. (34) and (35), which remain unchanged after letting $j_x^+ \to -j_x^-$, $j_x^- \to -j_x^+$, $m_y \to -m_y$, $\mu^+ \to \mu^-$ and $\mu^- \to \mu^+$. It is seen From Eqs. (37b) that the potential drop $\Delta\mu(m_y) = (\mu^- - \mu_c^0)$ is the same for $m_y = \pm 1$, and, hence, the two-terminal resistance measured between the FM and the TI surface, as shown in Fig. 3(b), remains the same irrespective of the magnetization direction of the FM, satisfying Onsager reciprocity. From Eq. (37a), we find that the potential drop $\Delta\mu(m_y) = (\mu_c^0 - \mu^+)$, as shown in Fig. 3(d), depends on the sign of m_y. Similarly, from Eqs. (37a) and (37b), we find that the potential drop $\Delta\mu(m_y) = (\mu^- - \mu^+)$, as shown in Fig. 3(f), depends on the sign of m_y. So the three-terminal resistances, as shown in Figs. 3(e) and 3(f), will depend on the magnetization direction of the FM contact, and $\delta\mu = \eta l_{\rm tr} I/\sigma W$ for both cases.

In the measurement setups shown in Figs. 3(g)–3(h), a current I is passed on the TI surface from the left of the FM contact to the right of the FM contact, and no current is injected or extracted through the FM contact, hence, $j_x^+ = j_x^- = I/W$. Then, we find the solution for μ^+ and μ^- to be

$$\mu^+ = \mu_c^0 - \left(1 - \frac{\eta^2 m_y^2}{2}\right)\frac{\xi IL}{2\sigma W} + \frac{\eta m_y l_{\rm tr}}{2\sigma}\frac{I}{W}, \quad \text{(38a)}$$

$$\mu^- = \mu_c^0 + \left(1 - \frac{\eta^2 m_y^2}{2}\right)\frac{\xi IL}{2\sigma W} + \frac{\eta m_y l_{\rm tr}}{2\sigma}\frac{I}{W}. \quad \text{(38b)}$$

The measurement setup shown in Figs. 3(g) and 3(h) are identical after an 180° rotation in the plane, so, the solution for the electrochemical potential on the TI surface given in Eqs. (38a) and (38b) (which is same as interchanging μ^+ and μ^-) are related after a change of sign of both I and m_y. The second term in both Eqs. (38a) and (38b) is the resistive potential drops along the surface of the TI under the FM contact, and the third term in both Eqs. (38a) and (38b) is nontrivial and because of the spin-momentum locking of the TI surface states. For the geometry of Fig. 3(g), we obtain the potential drop $\Delta\mu(m_y) = (\mu_c^0 - \mu^+)$ from Eq. (38a), and for the geometry of Fig. 3(h), we obtain the potential drop $\Delta\mu(m_y) = (\mu^- - \mu_c^0)$ from Eq. (38b), both of which depend on the sign of m_y. Therefore, the three-terminal resistances for the geometries of Figs. 3(g) and 3(h) will depend on the magnetization direction of the FM contact and could be used for spin detection with $\delta\mu = \eta l_{\rm tr} I/\sigma W$ for both cases.

Our results for $\delta\mu$ for three-terminal measurement geometries of Figs. 3(g) and 3(h) match with that of Hong *et al.* calculated in the limit of small tunneling for a FM point contact as a voltage probe on the TI surface [15], as well as that of Yokoyama *et al.* obtained after a perturbative solution of the coupled transport equations of the TI-FM bilayer with tunneling treated as perturbation [16]. From Eqs. (38a) and (38b), we also find that the potential drop $\Delta\mu(m_y) = (\mu^- - \mu^+)$ across the TI surface is independent of the sign of m_y, which also is consistent with the result by Yokoyama *et al.* [16]. The circuit pair shown in Figs. 3(c) and 3(d), the pair shown in Figs. 3(e) and 3(g), and the pair shown in Figs. 3(f) and 3(h) are reciprocal pairs. The resistance of each of these circuits can be calculated from Eqs. (36)–(38). For each reciprocal circuit pair, the Onsager reciprocity relation $R_1(+m_y) = R_2(-m_y)$ is satisfied, where R_1 and R_2 are m_y-dependent resistances of reciprocal circuits in each pair.

D. Consideration of nonzero length FM contact and importance of the tunnel barrier

We started with the quantum kinetic equation given in Eq. (1) which is derived under the gradient expansion assuming that the $\mathbf{r}$ and t dependence of the Green's function $g(\mathbf{r}, t; p_F\hat{\mathbf{p}}, \varepsilon)$ is smooth in the Fermi scale, i.e., $q_x \ll p_F$ and $\omega\tau_p \ll p_F l_p$. Furthermore, Eqs. (30) and (31) are derived from the matrix equation Eq. (29) after approximating $f_2 \approx 2\Omega$ under low-frequency long-wavelength diffusive limit assumption, $\omega\tau_p \ll 1$ and $q_x l_p \ll 1$. The assumptions in the gradient expansion and diffusive limit imply that the charge electrochemical potential μ on the TI surface varies smoothly on the scale of momentum relaxation length on the TI surface. In the solution of Eqs. (34) and (35), which are derived assuming δ function tunneling, μ has a discontinuity. However, the solution of μ in Eqs. (36)–(38) must be treated as the solution in the limiting case of the length of the FM contact becoming zero. Also, in experiment, the size of the contact is nonzero and at least an order of magnitude larger than the momentum relaxation length on the TI surface. Hence, the coupled transport equations, Eqs. (32) and (33), which are derived considering diffusive transport on the TI surface under the FM contact region, need to be resolved for a nonzero contact length. However, and as we will show do, these results for nonzero contact length continue to follow the Onsager reciprocity relation, and converge back to the corresponding line contact result, $\delta\mu = \eta l_{\rm tr} I/\sigma W$ in the limit of $L \to 0$. However, it is only beyond the line contact limit that we capture the importance of the tunnel contact in such spin-detection experiments.

The second order differential equation for the electrochemical potential μ on the TI surface under the FM contact is obtained by substituting Eq. (33) into Eq. (32). Since the FM contact is metallic with a conductivity much higher than the conductivity of the TI surface, the electrochemical potential of the FM $\mu_c(x)$ can be taken to be constant within the FM contact, i.e., $d_x\mu_c(x) = 0$ and $\mu_c(x) = \mu_c^0$ [37]. We define $\mu' = \mu - \mu_c^0$ to be the electrochemical potential on the TI surface with respect to the FM contact. Then, the equations for μ' and the current density j_x on the TI surface become

$$d_x^2\mu' - 2bm_y\, d_x\mu' + \left(b^2 m_y^2 - c^2\right)\mu' = 0, \quad \text{(39a)}$$

$$j_x = -\sigma'[\, d_x\mu' - bm_y\mu'], \quad \text{(39b)}$$

where $b = \xi\eta/l_{\rm tr}$ and $c = \sqrt{2\xi(1+\xi)}/l_{\rm tr}$. From Eq. 39, if $\mu'(j)$ is a solution given a current density j on the TI surface, then $\mu'(\alpha j) = \alpha\mu'(j)$ is also a solution. So, the potential difference $(\mu_1 - \mu_2) = (\mu_1' - \mu_2')$ between any two points 1 and 2 on the TI surface, or the potential difference $(\mu - \mu_c^0) = \mu'$ between any point on the TI surface and the FM, will be directly proportional to the current density, implying a linear current-voltage relationship. Also, from Eq. (39), after letting $x \to -x$ and $m_y \to -m_y$, either $j_x \to -j_x$ or $\mu' \to -\mu'$ indicting a symmetry of the problem under an 180° rotation in the plane. However, to check for Onsager reciprocity, we must solve Eq. (39) given specific boundary

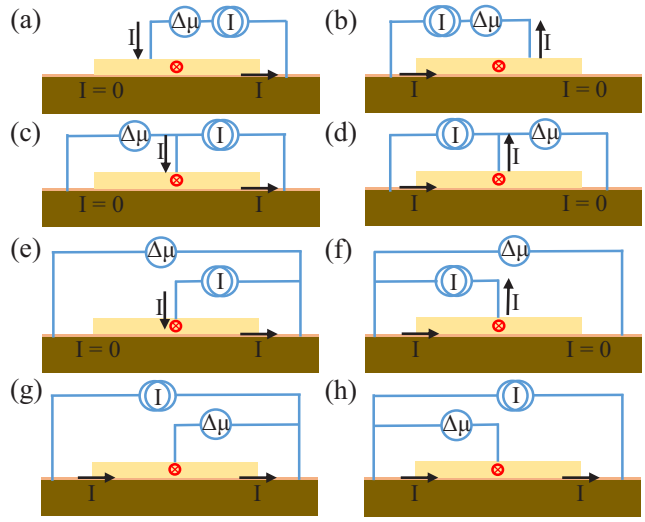

FIG. 4. Schematics of the cross-sectional view of 1D measurement geometries on the surface of a diffusive TI in the vicinity of the FM in the circuits of Fig. 1.

conditions associated with the reciprocal circuit pairs. The solution of μ' in Eq. (39a) is given by $\mu' = A_1 e^{r_1 x} + A_2 e^{r_2 x}$, where $r_{1,2} = bm_y \pm c$, and the unknown constants $A_{1,2}$ will be determined from the boundary conditions on j_x, which can be written as $j_x = -\sigma' c(A_1 e^{r_1 x} - A_2 e^{r_2 x})$ from Eq. (39b). To keep the notation consistent with that of a line contact in the limit $L \to 0$, we denote the electrochemical potentials on the TI surface to the left of the FM contact to be $\mu^- = \mu(x = 0)$ and the electrochemical potentials on the TI surface to the right of the FM contact to be $\mu^+ = \mu(x = L)$. In the following, we find the solutions for μ^+ and μ^- for specific geometries and discuss the linear current-voltage characteristic, the symmetry under an 180° rotation in the plane, the spin-detection voltage on the TI surface, the validity of the Onsager reciprocity relation and the importance of the tunnel barrier in such spin-detection experiments.

We first consider the case in which a current I is injected from the FM to the TI and extracted from one end or the other of the TI surface, as shown in Fig. 4. In the case in which the current is extracted from the right end on the TI surface as shown in Figs. 4(a), 4(c), and 4(e), the boundary conditions become $j_x(x = 0) = 0$ and $j_x(x = L) = I/W$. Then we obtain the solution for μ^+ and μ^- to be (see Appendix B)

$$\mu^+ = \mu_c^0 - \frac{I \coth(cL)}{\sigma' cW}, \tag{40a}$$

$$\mu^- = \mu_c^0 - \frac{I\,\mathrm{csch}(cL)}{\sigma' cW} e^{-bm_y L}. \tag{40b}$$

From Eq. (40a), the potential difference $\Delta\mu = (\mu_c^0 - \mu^+)$ does not depend on the magnetization direction of the FM. As a result, the two-terminal resistance measured between a FM and a NM contact of Fig. 4(a) will remain the same even after reversing the magnetization of the FM, satisfying the Onsager reciprocity relation. However, in the three-terminal measurement of Fig. 4(c) in which the potential at the leftmost point on the TI surface is measured with respect to the FM, the potential difference $\Delta\mu(m_y) = (\mu^- - \mu_c^0)$, which is found from Eq. (40b), depends on the magnetization direction of the FM. Similarly, in the three-terminal measurement of Fig. 4(e) in which the potential difference on the TI surface at the two ends is measured, $\Delta\mu(m_y) = (\mu^- - \mu^+)$ from Eqs. (40a) and (40b), depends on the magnetization direction of the FM.

If a current I is injected on the TI surface from the left end and extracted through the FM contact of Figs. 4(b), 4(d), and 4(f), the boundary conditions will be $j_x(x = 0) = I/W$ and $j_x(x = L) = 0$. Then we obtain μ^+ and μ^- to be (see Appendix B)

$$\mu^+ = \mu_c^0 + \frac{I\,\mathrm{csch}(cL)}{\sigma' cW} e^{bm_y L}, \tag{41a}$$

$$\mu^- = \mu_c^0 + \frac{I \coth(cL)}{\sigma' cW}. \tag{41b}$$

Equation (41) can be obtained from Eq. (40) after reversing the direction of the injected current I and the magnetization direction m_y of the FM, and interchanging the rightmost and the leftmost potentials μ^+ and μ^-, which reflects the 180° rotation symmetry in the plane of the device. In the two-terminal case as shown in Fig. 4(b), the potential difference $\Delta\mu = (\mu^- - \mu_c^0)$ from Eq. (41b) is independent of the FM magnetization, so the two-terminal resistance will remain the same even after reversal of the magnetization direction of the FM. In the three-terminal case as shown in Fig. 4(d), the potential difference $\Delta\mu(m_y) = (\mu_c^0 - \mu^+)$ from Eq. (41a) depends on the magnetization direction of the FM. Similarly, in the three-terminal case as shown in Fig. 4(f), the potential difference $\Delta\mu(m_y) = (\mu^- - \mu^+)$, which is obtained from Eqs. (41a) and (41b), also depends on the magnetization direction of the FM. Hence, in the three-terminal geometries of Figs. 4(c)–4(f), there will be a change of resistance under the magnetization reversal of the FM, which can be used for spin detection on the surface of a TI.

In the circuit geometries shown in Figs. 4(g)–4(h), the same current I is injected in and out of the two ends of the TI surface, and the boundary conditions are $j_x(x = 0) = j_x(x = L) = I/W$. Then, μ^+ and μ^- are given by (see Appendix B)

$$\mu^+ = \mu_c^0 - \frac{I\,\mathrm{csch}(cL)}{\sigma' cW}[\cosh(cL) - e^{bm_y L}], \tag{42a}$$

$$\mu^- = \mu_c^0 + \frac{I\,\mathrm{csch}(cL)}{\sigma' cW}[\cosh(cL) - e^{-bm_y L}]. \tag{42b}$$

From Eq. (42), under the reversal (change of sign) of both the direction of the injected current I and the FM magnetization direction m_y, the potentials on the rightmost and the leftmost points, μ^+ and μ^-, are interchanged, which again is due to the 180° rotation symmetry in the plane of the device. In the geometries of Figs. 4(g) and 4(h), the potential difference $\Delta\mu(m_y) = (\mu_c^0 - \mu^+)$ and $\Delta\mu(m_y) = (\mu^- - \mu_c^0)$, respectively, can be obtained from Eqs. (42a) and (42b). In both these cases, $\Delta\mu(m_y)$ depends on the magnetization direction of the FM and will change upon reversing the FM magnetization direction. However, the potential difference $\Delta\mu(m_y) = (\mu^- - \mu^+)$ is independent of the magnetization direction of the FM, which is consistent with the Onsager reciprocity relation, and the result by Yokoyama *et al.* [16].

All the potential differences, $\Delta\mu = (\mu_c^0 - \mu^+)$, $\Delta\mu = (\mu^- - \mu_c^0)$, and $\Delta\mu = (\mu^- - \mu^+)$, given by Eqs. (40)–(42), are proportional to the current I, implying a linear regime of the transport. The circuit geometries shown in Figs. 4(c) and

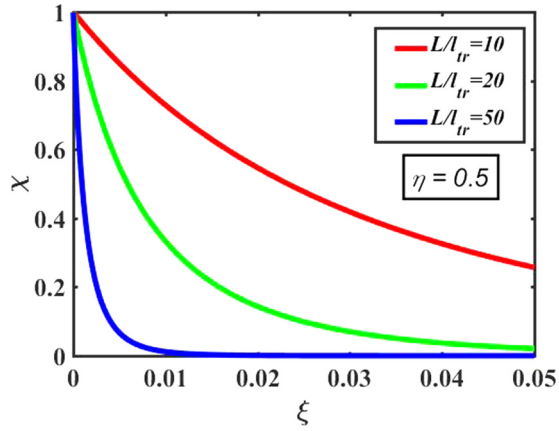

FIG. 5. Variation of the spin-detection efficiency χ with the normalized conductivity ξ of the FM tunnel contact on the surface of a diffusive TI for different values of the FM contact length L relative to the transport relaxation length $l_{\rm tr}$ on the TI surface.

4(d), Figs. 4(e) and 4(g), and Figs. 4(f) and 4(h) are reciprocal pairs with the voltage and the current terminals interchanged. In all these reciprocal circuit pairs, the resistance can be calculated using Eqs. (40)–(42), and in all the cases the Onsager reciprocity relation $R_1(+m_y) = R_2(-m_y)$ is satisfied, where R_1 and R_2 are the m_y dependent resistances of reciprocal circuits in each pair. In all the cases shown in Figs. 4(c)–4(h) using Eqs. (40)–(42), we find that the spin-detection voltage, $\delta\mu = [\Delta\mu(m_y = +1) - \Delta\mu(m_y = -1)]$, is given by

$$\delta\mu = \frac{2I}{\sigma' cW}\sinh(bL)\,\mathrm{csch}(cL). \tag{43}$$

From Eq. (43), in the limit $L \to 0$, we find that $\delta\mu = \eta I l_{\rm tr}/\sigma W$, which is the same as that obtained assuming tunneling from a δ function for the FM line contact, and that $\delta\mu$ is, indeed, independent of the conductance of the FM tunnel contact. Only for nonzero length FM contact, does $\delta\mu$ depend on the tunneling conductance of the FM contact. For small tunnel conductance, the Taylor series expansion of $\delta\mu$ for small values of ξ gives $\delta\mu = (\eta I l_{\rm tr}/\sigma W)[1 - \xi(L^2/3l_{\rm tr}^2)]$. So, in the limit $\xi \to 0$, we also obtain $\delta\mu = \eta I l_{\rm tr}/\sigma W$, which is independent of the length of the FM contact. We define the efficiency χ of the tunnel barrier as $\chi = \frac{\delta\mu(\xi)}{\delta\mu(\xi\to 0)}$. Therefore, the spin-detection voltage can be written as $\delta\mu(\xi) = \chi\eta I l_{\rm tr}/\sigma W$. In the limit $L \to 0$ or $\xi \to 0$, we have $\chi \to 1$. Figure 5 shows how χ changes with ξ for different values of $L/l_{\rm tr} = 10, 20, 50$, and $\eta = 0.5$. We have observed that the dependence of χ on η is negligible in the range of interest of the ξ and $L/l_{\rm tr}$ values, so the variation of χ with ξ for only $\eta = 0.5$ is shown. From Fig. 5 we can see that the spin-detection efficiency of the tunnel contact decreases as the conductivity of the FM contact increases. Also, the spin-detection efficiency of the FM contact decreases as the length of the FM contact increases. So the ideal contact for spin detection would be a FM line contact. However, in experiments, the FM contact has a nonzero and often substantial length compared to the transport relaxation length $l_{\rm tr}$ on the TI surface, and a tunnel barrier is needed to increase the spin-detection efficiency of the contact, which has been demonstrated in the experiments [2–14].

E. Consideration of NM contacts

The analysis of the circuit geometries shown in Figs. 1 and 2 with nonzero size contacts of length L can be performed using the circuit diagrams of Fig. 4 and with the help of Eqs. (40)–(42). However, to calculate the resistances for these circuit geometries, the potential drops due to both the FM and the NM contacts and the potential drop on the TI surface between the contacts must be considered. The potential drop on the TI surface between two contacts can be found by solving Eq. (28). If a constant current I flows on the surface of the TI from point 1 to point 2, the potential drop between the two points, 1 and 2, will be $\Delta\mu = (\mu_1 - \mu_2) = IL_{12}/\sigma W$, where L_{12} is the length between points 1 and 2. The potential drop due to the NM contact can be calculated considering the transport on the TI surface under the NM contact. Previously [36], we calculated the modified transport equations on the TI surface due to tunneling from the NM contact. In the 1D case, considering the transport on the TI surface along the x direction, the modified continuity equation of the TI surface states due to tunneling to and from the NM is given by [36]

$$d_x j_x = 2\gamma N_{\rm m}(e^2 N\mu_{\rm c} - n), \tag{44}$$

where $N_{\rm m}$ is the per spin DOS of the NM at the Fermi energy, and $\mu_{\rm c}$ is the charge electrochemical potential in the NM. In our previous work [36], we defined the interface transmission time $\tau_{\rm t}$ by $1/\tau_{\rm t} = \gamma N_{\rm m}$. The modified diffusion equation for the charge current density on the TI surface due to tunneling from the NM is given by [36]

$$j_x = \frac{1}{(1 + 4\gamma N_{\rm m}\tau_{\rm p})}\left[-v_{\rm F}^2\tau_{\rm p}\partial_x n - e^2\gamma N_{\rm m} N v_{\rm F}\tau_{\rm p}\mu_{\rm s}^y\right], \tag{45}$$

where $\mu_{\rm s}^y$ is the y component of the spin electrochemical potential in the NM [38]. From Eq. (44) we obtain the following modified continuity equation of the charge density on the TI surface under the NM,

$$d_x j_x = \frac{2\xi\sigma}{l_{\rm tr}^2}(\mu_{\rm c} - \mu). \tag{46}$$

For $\mu_{\rm s}^y = 0$, from Eq. (45), we obtain the following modified diffusion equation for the current density on the surface of the TI under the NM,

$$j_x = -\frac{\sigma}{(1 + \xi)}\, d_x\mu. \tag{47}$$

In case of the NM, we have $N_\uparrow = N_\downarrow = N_{\rm m}$, and, thus, $N_- = 0$, $N_+ = 2N_{\rm m}$; therefore, $\eta = 0$ and $\xi = 4\gamma N_{\rm m}\tau_{\rm p}$. Equations (46) and (47) also can be obtained from Eqs. (32) and (33), respectively, after letting $\eta = 0$ for the NM. So, to calculate the potential drops due to the nonzero length NM contact in Figs. 1 and 2, Eqs. (40)–(42) can be used after substituting $\eta = 0$.

The resistive potential drop on the TI surface and the resistive drop due to the NM contacts are independent of magnetization direction of the FM contact, and satisfy the Onsager reciprocity relation independently. Therefore, it is sufficient to consider the potential drop due to the FM contacts, as shown in Fig. 4, to check the validity of the Onsager reciprocity relation in multiterminal measurements as shown in Fig. 1 and the two-terminal measurements as shown in

Fig. 2. Considering the transport on the TI surface under the nonzero length FM contact, we have shown that the Onsager reciprocity relation is satisfied in spin-detection experiments on the surface of a TI, and how the conductivity of the FM tunnel contact affects the efficiency of the spin detection. Our conclusions remain valid even after considering detailed calculation of the potential drops due to all the other NM contacts and the drops on the TI surface between the contacts.

To illustrate how to include the potential drops considering the NM contacts of Figs. 1 and 2, we calculate the two-terminal resistances in the circuit geometries shown in Fig. 2 using the results obtained for the transport on the TI surface under the FM and the NM contact and the region in between the contacts. For the circuit geometries shown in Figs. 2(a) and 2(b), if the same current is flowed on the TI surface between the two contacts, the potential difference on the two contacts will be the sum of the potential drop due to the left contact, the potential drop on the TI surface in between the contacts, and the potential drop due to the right contact. The potential drop due to the left FM contact will be obtained from Eq. (40a), the potential drop due to the right NM contact of Fig. 2(a) or the right FM contact of Fig. 2(b) will be obtained from Eq. (41b), and the potential drop on TI surface in between the contacts will be given by $\Delta\mu = IL_{12}/\sigma W$. For both cases shown in Figs. 2(a) and 2(b), the two-terminal resistances are the same and given by

$$R_{2t} = \frac{\coth(c_1 L_1)}{\sigma_1' c_1 W} + \frac{IL_{12}}{\sigma W} + \frac{\coth(c_2 L_2)}{\sigma_2' c_2 W}. \tag{48}$$

Here $c_i = \sqrt{2\xi_i(1+\xi_i)}/l_{\rm tr}$ and $\sigma_i' = \sigma/(1+\xi_i)$, where ξ_i is proportional to the conductance of the tunnel barrier for the ith contact, L_i is the length of the ith contact ($i = 1, 2$), and L_{12} is the length between the contacts. The resistance given by Eq. 48 is independent of the magnetization direction of the FM contact of Fig. 2(a) or the magnetization direction of either of the FM contacts of Fig. 2(b). Hence, R_{2t} satisfies the Onsager reciprocity relation. The calculation for all the circuits shown in Fig. 1 can be performed in a similar way.

F. Consideration of spin-valve-like geometries

We also consider spin-valve-like four-terminal measurement geometries with two adjacent FM and two nonadjacent NM contacts on the surface of a diffusive TI. Among all the possible circuit geometries with such contact configurations, two of them being the voltage probes and other two being the current probes, we find four possible contact geometries (two sets of reciprocal circuit pairs), as shown in Fig. 6, that manifest the effects of magnetic orientations of both the FMs on the four-terminal resistance. We also note that, if the two FM and the two NM contacts are identical in the devices shown in Fig. 6, there will be a rotational symmetry axis normal to the plane of the devices. In case of identical contacts in the devices shown in Figs. 6(a) and 6(b), from the calculations based on Eqs. (40)–(42) we obtain the relationship, $R_{4t}(+\vec{M}_1, +\vec{M}_2) = R_{4t}(-\vec{M}_1, -\vec{M}_2)$, where this relationship satisfies the symmetry under an 180° rotation in the plane of the devices. However, we obtain $R_{4t}(+\vec{M}_1, -\vec{M}_2) \neq R_{4t}(-\vec{M}_1, +\vec{M}_2)$ consistent with the equality being not guaranteed by any symmetry or the Onsager reciprocity relation. Similarly, in case of identical contacts in the circuits shown in Figs. 6(c) and 6(d), the four point resistances obtained from our calculations using Eqs. (40)–(42) satisfy $R_{4t}(+\vec{M}_1, +\vec{M}_2) = R_{4t}(-\vec{M}_1, -\vec{M}_2)$, but we also obtain $R_{4t}(+\vec{M}_1, -\vec{M}_2) = R_{4t}(-\vec{M}_1, +\vec{M}_2)$ consistent with the Onsager relation since the two symmetric reciprocal device structures are related by an 180° rotation in the plane. Other terminal connection possibilities are shown in Figs. 6(e) and 6(f), which are reciprocal circuit pairs. We find from the calculations using the Eqs. (40)–(42) that the four-terminal resistances will not depend on either of the magnetizations of the FM contacts. This behavior also has been verified experimentally [4,14] and was attributed to very short spin relaxation time, which is same as the momentum relaxation time on the surface of the TI due to spin-momentum helical locking. We could, in principle, extend our calculations to derive the multiterminal resistance for any number of contacts.

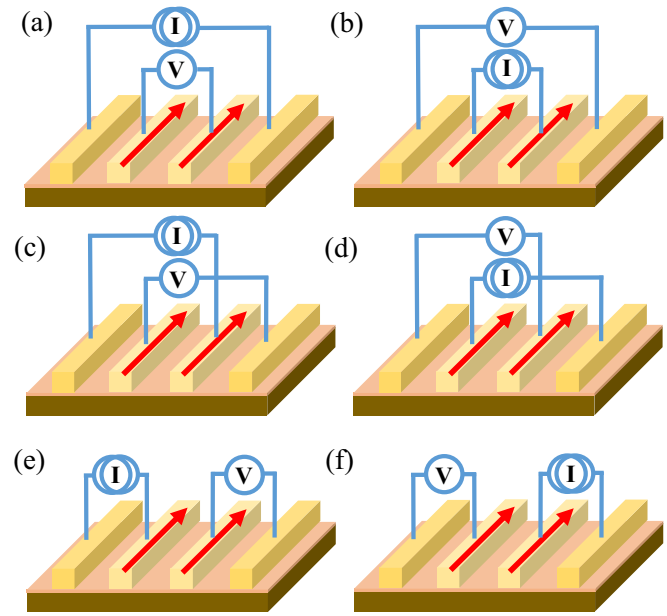

FIG. 6. Schematics of spin-valve-like measurement geometries with two FM contacts on the surface of a diffusive TI.

V. COMPARISON TO RESULTS IN THE LITERATURE

In this section, we first derive the spin-charge coupled transport equations of Burkov *et al.* [23], which was derived on the TI surface without any tunneling from the FM. Then, we show that the spin-charge coupled diffusion equations of Burkov *et al.* do not satisfy the continuity equation of the charge density, i.e., Eq. (26) in which the charge current density on the TI surface is given by Eq. (15).

To derive the transport on the TI surface in the case of no tunneling from the FM, we have $\gamma = 0$, hence, $h_2 = 0$, $\Omega = 1 - i\omega\tau_{\rm p}$ and $\Delta_x = {\rm q}_x v_{\rm F}\tau_{\rm p}$ in Eqs. (7), (8), and (9). Performing the ε integration of Eq. (7), we obtain

$$[\mathbb{I}_2 - \mathbb{D}_2]\rho_2 = 0, \tag{49}$$

where $\mathbb{I}_2$ is the 2×2 identity matrix and $\rho_2 = (n, 2s_y)^T$. The matrix $\mathbb{D}_2$ contains full information about the coupled spin

and charge transport on the TI surface. However, the matrix elements of $\mathbb{D}_2$ are complicated functions of Δ_x, Ω, and Ω_{so} as given in Eq. (8). Instead, to obtain the transport equations on the TI surface, we have multiplied Eq. (8) by $\mathbb{D}_2^{-1}$ to obtain the matrix equation Eq. (19), which gives Eq. (22) in case of no tunneling, and the matrix elements of $\mathbb{D}_2^{-1}$ are simple functions as given in Eq. (20). Moreover, as we have shown, the continuity equation of the charge density obtained from the matrix equation (22) remains true irrespective of the approximation made to obtain the second equation of the two coupled transport equations. The spin-charge coupled transport equations of Burkov *et al.* [23] can be obtained by approximating the matrix elements of $\mathbb{D}_2$ by invoking the diffusive approximations. The matrix equation (49) with the full matrix $\mathbb{D}_2$ satisfy the continuity equation of the charge density as we show below. However, we also show that it is quite nontrivial to approximate the matrix elements of $\mathbb{D}_2$ to get the spin-charge coupled diffusion equations from Eq. (49) such that the continuity equation of the charge density is satisfied even after the approximations.

First, we show that the spin-charge coupled diffusion equations on the TI surface without any tunneling from the FM satisfies the continuity equation of the charge density given the full matrix $\mathbb{D}_2$ in Eq. (8). Substituting $\mathbb{D}_2$ from Eq. (8) in Eq. (49) with $\Omega = 1 - i\omega\tau_p$ and $\Delta_x = q_x v_F \tau_p$, we obtain

$$\begin{bmatrix} 1-f_1 & -\frac{i}{\Delta_x}(1-\Omega f_1) \\ -\frac{i}{\Delta_x}(1-\Omega f_1) & 1-\frac{\Omega}{\Delta_x^2}(1-\Omega f_1) \end{bmatrix} \begin{bmatrix} n \\ 2s_y \end{bmatrix} = 0. \tag{50}$$

Multiplying Eq. (50) by the row vector $v_2 = (\Omega, -i\Delta_x)$ from the left gives Eq. (23), which is the continuity equation of the charge density expressed in the Fourier space. We observe that the equation $v_2[\mathbb{I}_2 - \mathbb{D}_2]\rho_2 = 0$ gives Eq. (23) if the full matrix $\mathbb{D}_2$ in Eq. (8) is used. Hence, we can obtain a constrain on how to expand the matrix elements of $\mathbb{D}_2$ such that the equation $v_2[\mathbb{I}_2 - \mathbb{D}_2]\rho_2 = 0$ continues to give Eq. (23), and thus the coupled spin-charge transport equations will satisfy the continuity equation for the charge density.

The matrix elements of $\mathbb{D}_2$ are expanded in series as

$$\begin{aligned} \mathbb{D}_{00} &= \frac{1}{\Omega} - \frac{\Delta_x^2}{2\Omega^3} + \frac{3\Delta_x^4}{8\Omega^5} + \cdots, \\ \mathbb{D}_{0y} = \mathbb{D}_{y0} &= \frac{i\Delta_x}{2\Omega^2} - \frac{3i\Delta_x^3}{8\Omega^4} + \cdots, \\ \mathbb{D}_{yy} &= \frac{1}{2\Omega} - \frac{3\Delta_x^2}{8\Omega^3} + \cdots. \end{aligned} \tag{51}$$

However, the approximations of the matrix elements of $\mathbb{D}_2$ have to be such that the equation $v_2[\mathbb{I}_2 - \mathbb{D}_2]\rho_2 = 0$ still give Eq. (23), which forces expanding each matrix element with different powers of Δ_x (or Ω) given by the following rule at each order of approximation: In the nth order, the rule is to keep the first $(n+1)$ terms of $\mathbb{D}_{00}$ and the first n terms in each of $\mathbb{D}_{0y}, \mathbb{D}_{y0}, \mathbb{D}_{yy}$ in Eq. (51). Hence, to the lowest order, one has to keep the first two terms of $\mathbb{D}_{00}$ and only the first term in each of $\mathbb{D}_{0y}, \mathbb{D}_{y0}, \mathbb{D}_{yy}$ in Eq. (51). For the next higher order, one has to keep the first three terms of $\mathbb{D}_{00}$ and the first two terms in each of $\mathbb{D}_{0y}, \mathbb{D}_{y0}, \mathbb{D}_{yy}$ in Eq. (51).

Previously [26], we had shown that the coupled spin-charge transport equations obtained by Burkov *et al.* [23] can be derived from Eq. (7) under the diffusive approximations. Here we precisely show that the transport equations of Burkov *et al.* are obtained after keeping the first two terms in both $\mathbb{D}_{00}$ and $\mathbb{D}_{yy}$ and the first term in both $\mathbb{D}_{0y}$ and $\mathbb{D}_{y0}$ in Eq. (51), which do not satisfy the above rules. However, we obtain

$$\begin{aligned} \mathbb{D}_{00} &= (1 - i\omega\tau_p)^{-1} - \frac{\Delta_x^2}{2}(1 - i\omega\tau_p)^{-3} \\ &\approx 1 + i\omega\tau_p - \frac{q_x^2 v_F^2 \tau_p^2}{2}, \\ \mathbb{D}_{0y} = \mathbb{D}_{y0} &= \frac{i\Delta_x}{2}(1 - i\omega\tau_p)^{-2} \approx \frac{iq_x v_F \tau_p}{2}, \\ \mathbb{D}_{yy} &= \frac{1}{2}(1 - i\omega\tau_p)^{-1} - \frac{3\Delta_x^2}{8}(1 - i\omega\tau_p)^{-3} \\ &\approx \frac{1}{2}(1 + i\omega\tau_p) - \frac{3q_x^2 v_F^2 \tau_p^2}{8}. \end{aligned} \tag{52}$$

In deriving the approximate values of the matrix elements, we have neglected terms of order $\omega^2\tau_p^2$, $\omega\tau_p q_x l_p$ and higher. Substituting the values from Eq. (52) into Eq. (49), we obtain

$$\begin{bmatrix} -i\omega\tau_p + \frac{1}{2}q_x^2 v_F^2 \tau_p^2 & -\frac{1}{2}iq_x v_F \tau_p \\ -\frac{1}{2}iq_x v_F \tau_p & \frac{1}{2} - \frac{1}{2}i\omega\tau_p + \frac{3}{8}q_x^2 v_F^2 \tau_p^2 \end{bmatrix} \begin{bmatrix} n \\ 2s_y \end{bmatrix} = 0. \tag{53}$$

Equation (53) is exactly what we derived in our prior work [26]. After inverse Fourier transforming Eq. (53) to real space, the following coupled spin-charge transport equations of Burkov *et al.* [23] are obtained,

$$\partial_t n = D_0 \partial_x^2 n + 2\Gamma \partial_x s_y, \tag{54a}$$

$$\partial_t s_y = \frac{3D_0}{2}\partial_x^2 s_y - \frac{s_y}{\tau_p} + \Gamma \partial_x n, \tag{54b}$$

where $D_0 = v_F^2\tau_p/2$ was the diffusion constant, and $\Gamma = v_F/2$ was the spin-charge coupling constant. It should be noted that diffusion constant $D_0 = v_F^2\tau_p/2$ indicates that the momentum relaxation time is τ_p instead of $2\tau_p$. Similarly, Eq. (54b) indicates that the spin relaxation time is also τ_p instead of $2\tau_p$. The mismatch of a factor of 2 in both the the momentum relaxation time and the spin relaxation time from the actual values is an indication of the inaccuracy of the coupled spin-charge transport equations of Burkov *et al.*

Since, the matrix elements of $\mathbb{D}_2$ given in Eq. (52) were not derived according to the above rules for order of approximation, the transport equation Eq. (54a) is inconsistent with the continuity equation of the charge density given in Eq. (26), if the actual charge current density given in in Eq. (15), i.e., $j_x = -2v_F s_y$, is considered. Alternatively, if the charge current density is defined from the transport equation, Eq. (54a), after considering Eq. (54a) as the continuity equation of the charge density, as what was done by Burkov *et al.* [23], the resulting new definition of the charge current density, $j_x = -D\partial_x n - 2\Gamma s_y$, becomes inconsistent with the actual charge current density given in Eq. (15). However, if the second order $\partial_x^2 s_y$ term in Eq. (54b) is neglected, as described by the above rules, $s_y = \Gamma\tau_p\partial_x n$ is obtained in steady state. Substituting $s_y = \Gamma\tau_p\partial_x n$ in Eq. (54a) results in $\partial_t n - 2v_F\partial_x s_y = 0$, and

we recover the charge continuity equation $\partial_t n + \partial_x j_x = 0$ with $j_x = -2v_F s_y$.

Here, based on a derivation from the quantum kinetic equation, we show that the spin-charge coupled transport equations for the TI surface states obtained by Burkov *et al.* [23] are inconsistent with the continuity equation of the charge density. Burkov *et al.* [23] derived the spin-charge coupled transport equation from the density response function formalism using standard perturbation theory. It can be shown similarly, though it is beyond the scope of this paper, that the expansion in terms of the small parameters $\omega\tau_p$, $q_x l_p$, in that formalism too has to be such that the resulting transport equations are consistent with the continuity equation of the charge density, for the charge conservation to hold, even after making standard current conserving approximations for the Green's function and the self-energy in perturbation theory.

Schwab *et al.* had calculated the resistance between a FM line contact and a point on the TI surface using Eq. (32) and ignoring Eq. (33), and the result did violate Onsager reciprocity. We have shown that considering both Eqs. (32) and (33), indeed, results in the two-terminal resistance that satisfies Onsager reciprocity, even in the case of FM line contact. However, ignoring Eq. (33), as Schwab *et al.* [24] did, does lead to the violation of the Onsager reciprocity relation.

Previously, Sayed *et al.* [19] had addressed the issue of Onsager reciprocity in multiterminal spin-valve-like measurements on the surface of a diffusive TI by deriving the resistance from the solution of a phenomenological one-dimensional diffusion equation in terms of electrochemical potentials of four propagating channels on the surface of the TI, where each channel corresponds to a specific combination of spin orientation (up and down) and direction of propagation (right and left moving), and modeling the FM and NM contacts on the TI surface as line contacts [18,19]. However, Sayed *et al.* [19] only considered specific cases as those of Figs. 1(a) and 1(b), Fig. 2(b), and Figs. 6(a) and 6(b). Our finding matches with the ones obtained by Sayed *et al.* [19] in the case of Figs. 1(a) and 1(b) and Figs. 6(a) and 6(b) with both the FM contacts being considered identical. However, in the case of two-terminal resistance between the two FM contacts as shown in Fig. 2(b), the result of Sayed *et al.* [19] obeyed the Onsager reciprocity relation, i.e., $R_{2t}(+\vec{M}_1, +\vec{M}_2) = R_{2t}(-\vec{M}_1, -\vec{M}_2)$ and $R_{2t}(+\vec{M}_1, -\vec{M}_2) = R_{2t}(-\vec{M}_1, +\vec{M}_2)$, but with the relation $R_{2t}(+\vec{M}_1, +\vec{M}_2) \neq R_{2t}(+\vec{M}_1, -\vec{M}_2)$ instead of R_{2t} being independent of both the magnetization directions of the FM contacts that we have derived in Eq. (48). In our model, the TI is purely diffusive and all the spin information is lost after a few momentum scattering events on the TI surface. The loss of information of the spin of electrons (or the information of the magnetizations of the FM contacts) from the two injecting FM contacts is due to the spin-momentum helical locking of the TI surface states, where each momentum scattering also randomizes the spin which is locked to the momentum of the TI surface states. Hence, we find that the two-terminal resistance R_{2t} given in Eq. (48) does not depend on either of the FM magnetization directions. It might be the case that the result obtained by Sayed *et al.* [19] is an outcome of their model not being purely diffusive, but only based on a phenomenological diffusion equation of individual spin up and spin down propagation modes, where the spin information is not completely lost even after a significant number of momentum scattering events (although they had to introduce spin-flip scattering artificially to account for that). By contrast, in our theory, the transport equations on the surface of a TI are derived starting from the quantum kinetic equation under diffusive approximations. We believe that the two-terminal resistance between two FM on the surface of a TI in ballistic transport regime will satisfy relations, $R_{2t}(+\vec{M}_1, +\vec{M}_2) = R_{2t}(-\vec{M}_1, -\vec{M}_2)$, $R_{2t}(+\vec{M}_1, -\vec{M}_2) = R_{2t}(-\vec{M}_1, +\vec{M}_2)$, but $R_{2t}(+\vec{M}_1, +\vec{M}_2) \neq R_{2t}(+\vec{M}_1, -\vec{M}_2)$, resembling that of Sayed *et al.* [19].

The two-terminal resistance between a FM and a NM contact on the surface of a ballistic TI was calculated theoretically by Gotte *et al.* [27], but the calculated theoretical result apparently violates the Onsager reciprocity relation. In the ballistic transport regime, the probability conservation law, i.e., the conservation of charge density, along with the time reversal symmetry, which is achieved by reversing the magnetization direction of the FM, ensures a symmetry of the conductance matrix such that the Onsager reciprocity relation is satisfied in the linear response regime. The calculation for the pure ballistic case to establish the validity of the Onsager reciprocity relation is beyond the scope of this current work. Nevertheless, Semenov *et al.* [28] had understood that the Onsager reciprocity will be satisfied in both the ballistic and the diffusive case, and, hence, they proposed a phenomenological model for the quasiballistic mesoscopic regime in which they showed that the reciprocity and even the linear current-voltage relationship around the zero bias are violated. However, a detailed formal derivation based on transmission matrix method similar to that of Buttiker [22], or a calculation based on the quantum kinetic equation, is needed to test such violation of Onsager reciprocity in the mesoscopic regime of transport.

In the experiment, the transport regime is mostly diffusive, hence the observation of different two-terminal resistance with reversal of FM magnetization direction still needs to be explained. Very recently, Tian *et al.* [39] observed spin memory effect in three-terminal spin detection experiments on the surface of a TI and postulated that one possible reason for the observed spin memory effect might be the hyperfine interaction between the nuclear spin in the atom and the conduction electron spin, in which atomic nuclear spin has a much larger lifetime giving rise to a memory effect. In case of two-terminal magneto-resistance experiment involving FM contacts on the surface of a TI, such hyperfine interaction could similarly give rise to change of resistance upon magnetic field reversal. Since the nuclear spin in the atom does not relax to become reversed with the reversal of the FM magnetization, the Onsager reciprocity relation could not be applied, since application of the Onsager reciprocity relation requires time reversal invariance, which is achieved by reversing all the internal magnetic moments and the external magnetic fields in the system. In this work, we have shown that in the purely diffusive regime of transport, the Onsager reciprocity relation is maintained, which contrasts to prior results that also assumed diffusive transport but found violations of Onsager reciprocity for reasons detailed before. This work, therefore, suggests that the apparent violations of

the Onsager reciprocity relation in the experiments must have a different source.

VI. CONCLUSION

In summary and conclusion, starting from the quantum kinetic equation, we have derived the diffusive transport equations on the surface of a TI coupled to a FM to explain two-terminal and multiterminal spin detection measurements on the TI surface. In the kinetic equation, the effect of the FM tunnel contact on the transport has been considered by taking into account a self-energy due to tunneling across the TI-FM interface that acts as a source term in the charge transport equations of the carriers on the surface of the TI under the FM tunnel contact. The diffusion equations are solved analytically to calculate the change in chemical potential in the TI and the FM due to the charge current on the TI surface for different measurement geometries. Based on our analytical model, we define a spin-detection voltage as the change in voltage measured on the FM contact on reversing the FM magnetization direction. We find that the spin-detection voltage depends on the DOS polarization of the FM, the amount of charge current on the TI surface and the conductivity of the tunnel contact. We show that the spin-detection voltage decreases with increasing tunnel conductivity of the tunnel barrier. We also show that the Onsager reciprocity relation is satisfied in both the two-terminal and multiterminal spin-detection experiments on the surface of a diffusive TI, which resolves conflicting issues in prior literature, as well as explains the results of multiterminal spin-detection experiments on the surface of a diffusive TI. Our results suggest that the experimental findings of two-terminal resistance that depends on the FM magnetization direction need further interpretation.

ACKNOWLEDGMENT

This work is supported by NSF under the grant NNCI ECCS-1542159 and NASCENT ERC.

APPENDIX A: DERIVATION OF THE QUANTUM KINETIC EQUATION

To derive the quantum kinetic equation describing transport on the TI surface coupled to the FM, we follow our previous papers [34,36]. We consider the following total Hamiltonian for the TI-FM heterostructure of Fig. 4,

$$H_{\rm tot} = H_{\rm TI} + H_{\rm dis} + H_{\rm FM} + H_{\rm tun}. \tag{A1}$$

Here $H_{\rm TI}$ is the low-energy effective Hamiltonian for the TI surface states in second-quantized form, which is given by

$$H_{\rm TI} = \lambda \int d^2{\rm R} \sum_{\alpha,\beta} c^\dagger_\alpha(\mathbf{R})[\varepsilon_{\rm TI}(\mathbf{R}) - \varepsilon_{\rm F}\sigma_0 - e\phi\sigma_0]_{\alpha\beta} c_\beta(\mathbf{R}), \tag{A2}$$

where $\varepsilon_{\rm TI}(\mathbf{R}) = -i\hbar v_{\rm F}[(\nabla_{\mathbf{R}} \times \hat{\mathbf{z}})\cdot\boldsymbol{\sigma}]$, $v_{\rm F}$ is the Fermi velocity of the Dirac surface states, $\varepsilon_{\rm F}$ is the Fermi energy, ϕ is the electrostatic potential of any electric field ($\mathbf{E} = -\nabla_{\mathbf{R}}\phi$) on the TI surface, and $\mathbf{R}$ is the 2D position vector on the TI surface. The creation and annihilation operators of the TI surface states are $c^\dagger_\alpha(\mathbf{R})$, $c_\beta(\mathbf{R})$ (where (α,β) are the spin indices) which satisfy the equal-time anticommutator relation $\{c_\alpha(\mathbf{R}), c^\dagger_\beta(\mathbf{R}')\} = \lambda^{-1}\delta(\mathbf{R}-\mathbf{R}')\delta_{\alpha\beta}$ normalized to the thickness λ of the TI surface states. The disorder Hamiltonian $H_{\rm dis}$ representing the impurities on the TI surface is given by

$$H_{\rm dis} = \lambda \int d^2{\rm R} \sum_\alpha c^\dagger_\alpha(\mathbf{R}) V_{\rm dis}(\mathbf{R}) c_\alpha(\mathbf{R}), \tag{A3}$$

where $V_{\rm dis}(\mathbf{R}) = V_{\rm d} a_{\rm d} \Sigma_{j=1}^{N_{\rm I}} \delta(\mathbf{R} - \mathbf{R}^{\rm I}_j)$ is the spin-independent short-ranged impurity potential, $V_{\rm d}$ is the average impurity potential for impurities on and close to the interface, $\mathbf{R}^{\rm I}_j$ are the locations of the randomly distributed impurities, and and $a_{\rm d}$ is a normalization constant with unit of area for the normalization of the δ function.

We consider the FM Hamiltonian $H_{\rm FM}$, which is given by

$$H_{\rm FM} = \int d^3{\rm r} \sum_{\alpha,\beta} d^\dagger_\alpha(\mathbf{r})[\varepsilon_{\rm FM}(\mathbf{r}) - \varepsilon_{\rm F}\sigma_0 - e\phi_{\rm c}\sigma_0]_{\alpha\beta} d_\beta(\mathbf{r}). \tag{A4}$$

Here, $\varepsilon_{\rm FM}(\mathbf{r}) = [-\frac{\hbar^2}{2m_{\rm c}}\nabla^2_{\mathbf{r}} + \varepsilon_{\rm b}]\sigma_0 - \Delta_{\rm ex}\mathbf{m}\cdot\boldsymbol{\sigma}$ describes the two spin-split bands in the FM, $\mathbf{r}$ is the 3D position vector in the metal, $m_{\rm c}$ is the effective mass for both the conduction bands in the FM, $\varepsilon_{\rm b}$ is the band offset relative to the Dirac point of the TI surface states, $\Delta_{\rm ex}$ is the effective strength of exchange interaction between the itinerant s-electrons and the localized d-electrons in the FM, $\mathbf{m}$ is the unit vector along the direction of magnetization in the FM and $\phi_{\rm c}$ is the electrostatic potential of any electric field in the FM. The two bands of the FM will be spin splitted with an splitting energy of $2\Delta_{\rm ex}$. The creation and annihilation operators in the metal are $d^\dagger_\alpha(\mathbf{r})$ and $d_\beta(\mathbf{r})$, which satisfy the equal-time anticommutator $\{d_\alpha(\mathbf{r}), d^\dagger_\beta(\mathbf{r}')\} = \delta(\mathbf{r}-\mathbf{r}')\delta_{\alpha\beta}$. The creation and the annihilation operators in the metal and on the TI surface anticommutes, i.e., $\{c_\alpha(\mathbf{R}), d^\dagger_\beta(\mathbf{r}')\} = 0$.

The coupling of the TI surface states to the FM is described by a tunneling Hamiltonian $H_{\rm tun}$, which represents the transmission of the electron in and out of the TI surface states from and to the FM, given by

$$H_{\rm tun} = \lambda \int d^2{\rm R} \int d^3{\rm r} \sum_{\alpha,\beta} [d^\dagger_\alpha(\mathbf{r}) T_{\alpha\beta}(\mathbf{r},\mathbf{R}) c_\beta(\mathbf{R}) + {\rm H.c.}]. \tag{A5}$$

We consider a site-to-site (local) instantaneous tunneling at the interface, and the tunneling matrix has the form $T_{\alpha\beta}(\mathbf{r},\mathbf{R}) = t_{\alpha\beta} f(\mathbf{R})\delta(\mathbf{r}_\parallel - \mathbf{R})\delta(z)$, where $t_{\alpha\beta} f(\mathbf{R})$ describes the nature of the tunneling. The dependence of $t_{\alpha\beta}$ on the spin indices $(\alpha\beta)$ describes whether the tunneling is spin-conserving or spin-selective but spin-nonconserving, and the dependence of $f(\mathbf{R})$ on $\mathbf{R}$ describes whether the tunneling is momentum-randomizing or in-plane momentum-conserving. In case of a rough interface, the tunneling will be momentum-randomizing, and the tunneling is modeled by randomly distributed tunneling centers with $f(\mathbf{R}) = a_{\rm t}\Sigma_{i=1}^{N_{\rm S}}\delta(\mathbf{R} - \mathbf{R}^{\rm S}_i)$, where $\mathbf{R}^{\rm S}_i$ are the positions of the tunneling centers, and $a_{\rm t}$ is a normalization constant with unit of area for the normalization of the δ function. In case of a smooth interface, the tunneling will be in-plane momentum-conserving, and the tunneling is modeled by a position-independent function $f(\mathbf{R})$ (we take $f(\mathbf{R}) = 1$). For spin-conserving tunneling, the tunneling can

be modeled by $t_{\alpha\beta} = t_0\delta_{\alpha\beta}$, where the tunneling from both the bands in the FM to the TI surface states (and vice versa) have the same tunneling strength t_0. For spin-selective but spin-nonconserving tunneling, the tunneling from the two bands in the FM to the TI surface states (and vice versa) will have a different strength, and the tunneling can be modeled by $t_{\alpha\beta} = (t_\uparrow \mathrm{P}_\uparrow + t_\downarrow \mathrm{P}_\downarrow)_{\alpha\beta}$. Here $\mathrm{P}_{\uparrow,\downarrow} = (\sigma_0 + \mathbf{m}\cdot\boldsymbol{\sigma})/2$ are the projection operators to the two spin split bands in the FM, and $t_{\uparrow,\downarrow}$ are the corresponding tunneling strength. If $t_\uparrow \neq t_\downarrow$, the tunneling will be spin-nonconserving, and the spin-conserving tunneling is a special case when $t_\uparrow = t_\downarrow = t_0$.

The quantum kinetic equation obtained from the Keldysh component of the Wigner transformed left-right subtracted Dyson equation after gradient expansion is given by [40]

$$\begin{aligned}\partial_t G^{\mathrm{K}} - e\,\partial_t\phi\,\partial_\varepsilon G^{\mathrm{K}} + \frac{1}{2}\{\mathbf{v}\cdot\boldsymbol{\nabla}_{\mathbf{R}}, G^{\mathrm{K}}\} \\ + e\,\boldsymbol{\nabla}_{\mathbf{R}}\phi\cdot\boldsymbol{\nabla}_{\mathbf{p}} G^{\mathrm{K}} + \frac{i}{\hbar}[\varepsilon_{\mathrm{TI}}(\mathbf{p}), G^{\mathrm{K}}] \\ = -i(\Sigma^{\mathrm{R}}G^{\mathrm{K}} - G^{\mathrm{K}}\Sigma^{\mathrm{A}}) + i(G^{\mathrm{R}}\Sigma^{\mathrm{K}} - \Sigma^{\mathrm{K}}G^{\mathrm{A}}).\end{aligned} \tag{A6}$$

Here $\varepsilon_{\mathrm{TI}}(\mathbf{p}) = \hbar v_{\mathrm{F}}(\mathbf{p}\times\hat{\mathbf{z}})\cdot\boldsymbol{\sigma}$, $\mathbf{v} = v_F(\hat{\mathbf{z}}\times\boldsymbol{\sigma})$, $G^{\mathrm{R,A,K}}$ and $\Sigma^{\mathrm{R,A,K}}$ are the the retarded (R), advanced (A), and Keldysh (K) component of the Wigner transformed Green's functions (G) for the TI surface states and the self-energies (Σ) in terms of the variable $(\mathbf{R}, t; \mathbf{p}, \varepsilon)$. Here, $(\mathbf{R}, t)$ are the center-of-mass position and time coordinates and $(\mathbf{p}, \varepsilon)$ are the Fourier transformed momentum and energy of the relative position and time coordinates. The self-energy has contributions from both disorder and tunneling Hamiltonian, i.e., $\Sigma = \Sigma_{\mathrm{dis}} + \Sigma_{\mathrm{tun}}$, where Σ_{dis} is the self-energy due to disorder impurity potential and Σ_{tun} is the self-energy due to tunneling from the FM to the TI surface states. We consider time-independent electric fields on the TI surface, hence, the electrostatic potential will be time-independent, i.e., $\partial_t\phi = 0$.

After impurity averaging, the self-energy for disorder is given by

$$\Sigma^{\mathrm{R,A,K}}_{\mathrm{dis}}(\mathbf{R}, t; \mathbf{p}, \varepsilon) = \frac{\lambda a_{\mathrm{d}}^2 V_{\mathrm{d}}^2 n_{\mathrm{i}}}{\hbar}\int \frac{d^2\mathrm{p}'}{(2\pi)^2} G^{\mathrm{R,A,K}}(\mathbf{R}, t; \mathbf{p}', \varepsilon), \tag{A7}$$

where n_{i} is the impurity concentration per unit area on the TI surface. We introduce the quasiclassical Green's function of the TI surface states,

$$g^{\mathrm{R,A,K}}(\mathbf{R}, t; \mathrm{p_F}\hat{\mathbf{p}}, \varepsilon) = \frac{i\lambda}{\pi}\int d\xi_{\mathrm{p}}\, G^{\mathrm{R,A,K}}(\mathbf{R}, t; \mathbf{p}, \varepsilon), \tag{A8}$$

where $\mathrm{p_F}$ is the Fermi momentum of the TI surface states, $\hat{\mathbf{p}}$ is the unit vector along $\mathbf{p}$, and $\xi_{\mathrm{p}} = \hbar v_{\mathrm{F}}|\mathbf{p}| - \varepsilon_{\mathrm{F}}$. In Eq. (A8) the integration is performed near the Fermi energy, and we assume that the Fermi energy is in the conduction band of the TI. Hence, only the projection of the Green's function of the TI surface states to the conduction band is relevant to the transport, which is

$$G^{\mathrm{R,A}}(\mathbf{p}, \varepsilon) = \frac{1}{2\lambda}\frac{\sigma_0 + (\hat{\mathbf{p}}\times\hat{\mathbf{z}})\cdot\boldsymbol{\sigma}}{\varepsilon - \xi_{\mathrm{p}} \pm i0^+}. \tag{A9}$$

So the quasiclassical Green's functions and the disorder self-energies are give by

$$\begin{aligned} g^{\mathrm{R,A}} &= \pm\frac{1}{2}[\sigma_0 + (\hat{\mathbf{p}}\times\hat{\mathbf{z}})\cdot\boldsymbol{\sigma}], \\ \Sigma^{\mathrm{R,A}}_{\mathrm{dis}} &= \mp\frac{i}{2\tau_{\mathrm{p}}}\sigma_0, \end{aligned} \tag{A10}$$

where τ_{p} is the scattering time between the Bloch states in the TI and is defined by $1/\tau_{\mathrm{p}} = \pi a_{\mathrm{d}}^2 V_{\mathrm{d}}^2 n_{\mathrm{i}} N/\hbar$, and N is the DOS of the TI surface states at the Fermi energy. Since the quasiclassical Green's function of the TI surface states will be peaked at the Fermi energy, we have

$$G^{\mathrm{K}}(\mathbf{R}, t; \mathbf{p}, \varepsilon) = -\frac{i\pi}{\lambda} g^{\mathrm{K}}(\mathbf{R}, t; \mathrm{p_F}\hat{\mathbf{p}}, \varepsilon)\delta(\xi_{\mathrm{p}}), \tag{A11}$$

and the Keldysh component of Σ_{dis} is given by

$$\Sigma^{\mathrm{K}}_{\mathrm{dis}}(\mathbf{R}, t; \mathbf{p}, \varepsilon) = -\frac{i}{\tau_{\mathrm{p}}}\langle g^{\mathrm{K}}(\mathbf{R}, t; \mathrm{p_F}\hat{\mathbf{p}}, \varepsilon)\rangle, \tag{A12}$$

where $\langle\cdot\rangle$ denotes angular averaging over the Fermi contour of the TI surface states.

In case of a rough interface, the retarded, advanced and Keldysh components of the tunneling self-energy $\Sigma^{\mathrm{R,A,K}}_{\mathrm{tun}} = \Sigma^{\mathrm{R,A,K}}_{\mathrm{tun}}(\mathbf{R}, t; \mathbf{p}, \varepsilon)$ are obtained after averaging over the random distribution of the tunneling centers, and momentum randomization happens in the tunneling process. As a result, the tunneling self-energy is given by

$$\Sigma^{\mathrm{R,A,K}}_{\mathrm{tun}} = \frac{\lambda a_{\mathrm{t}}^2 n_{\mathrm{s}}}{\hbar}\int \frac{d^3\mathrm{k}'}{(2\pi)^3}\tilde{t}^\dagger G^{\mathrm{R,A,K}}_{\mathrm{FM}}\tilde{t}, \tag{A13}$$

where n_{s} is the density of the tunneling centers per unit area, $G^{\mathrm{R,A,K}}_{\mathrm{FM}} = G^{\mathrm{R,A,K}}_{\mathrm{FM}}(\mathbf{R}, z = 0, t; \mathbf{k}', \varepsilon)$ are the retarded, advanced and Keldysh components of the Green's function of the FM at the interface $z = 0$ with $\mathbf{k}'$ being the 3D momentum in the FM, and $\tilde{t} = (t_\uparrow \mathrm{P}_\uparrow + t_\downarrow \mathrm{P}_\downarrow)$ is the spin-dependent part of the tunneling (note that $\tilde{t}$ is Hermitian, i.e., $\tilde{t}^\dagger = \tilde{t}$).

The retarded and advanced Green's functions of the FM are

$$G^{\mathrm{R,A}}_{\mathrm{FM}}(\mathbf{k}, \varepsilon) = \mathrm{P}_\uparrow\frac{1}{\varepsilon - \xi_{\mathrm{k}\uparrow} \pm i0^+} + \mathrm{P}_\downarrow\frac{1}{\varepsilon - \xi_{\mathrm{k}\downarrow} \pm i0^+}. \tag{A14}$$

where $\xi_{\mathrm{k}\uparrow,\downarrow} = \frac{\hbar^2}{2m_{\mathrm{c}}}\mathrm{k}^2_{\uparrow,\downarrow} + \varepsilon_{\mathrm{b}} \mp \Delta_{\mathrm{ex}} - \varepsilon_{\mathrm{F}}$. Considering incoherent superposition of up and down electrons in the FM, the Keldysh component of the Green's function of the FM, which will be peaked at the Fermi energy, can be written as

$$G^{\mathrm{K}}_{\mathrm{FM}} = -i\pi[\mathrm{P}_\uparrow\tilde{g}^{\mathrm{K}}_\uparrow(\mathrm{k_{F\uparrow}}\hat{\mathbf{k}}_\uparrow, \varepsilon)\delta(\xi_{\mathrm{k}\uparrow}) + \mathrm{P}_\downarrow\tilde{g}^{\mathrm{K}}_\downarrow(\mathrm{k_{F\downarrow}}\hat{\mathbf{k}}_\downarrow, \varepsilon)\delta(\xi_{\mathrm{k}\downarrow})], \tag{A15}$$

where $\tilde{g}^{\mathrm{K}}_{\uparrow,\downarrow}$ are the Keldysh components of the quasiclassical Green's functions for the up and down electrons in the FM, $\mathrm{k_{F\uparrow,\downarrow}}$ are the Fermi momentum of the up and down electrons in the FM, and in Eq. (A15) the position and time dependence of the Keldysh components of the Green's functions are implicit. It should also be noted that, the Keldysh component of the tunneling self-energy is given by the Keldysh component of the Green's function of the FM evaluated at the interface. However, the assumption of a constant Keldysh component of the Green's function of the FM with position inside the FM will be self-consistent (because the thickness of the FM is considered to be small and the conductivity of the FM is much

higher than the conductivity of the TI, and, after considering transport inside the FM it can be shown that the variation of the nonequilibrium up and down electrochemical potential of the FM with position inside the FM will be negligible [37]).

The retarded, advanced and Keldysh components of the tunneling self-energy become

$$\Sigma^{\mathrm{R,A}}_{\mathrm{tun}} = \mp i(\gamma_\uparrow N_\uparrow \mathrm{P}_\uparrow + \gamma_\downarrow N_\downarrow \mathrm{P}_\downarrow),$$
$$\Sigma^{\mathrm{K}}_{\mathrm{tun}} = -i(\gamma_\uparrow N_\uparrow \mathrm{P}_\uparrow g_\uparrow + \gamma_\downarrow N_\downarrow \mathrm{P}_\downarrow g_\downarrow), \tag{A16}$$

where $\gamma_{\uparrow,\downarrow} = \pi\lambda a_{\mathrm{t}}^2 t_{\uparrow,\downarrow}^2 n_{\mathrm{s}}/\hbar$ are the strengths of tunneling between the up and down spin electrons in the FM and the TI surface states, $N_{\uparrow,\downarrow}$ are the DOS of the up and down electrons in the FM at the Fermi energy, and $g_{\uparrow,\downarrow} = \langle \tilde{g}^{\mathrm{K}}_{\uparrow,\downarrow} \rangle$ denotes the value of the Keldysh component of the quasiclassical Green's function for the up and down electrons in the FM after averaging over the solid angle of the respective Fermi surfaces of each spin bands in the FM.

In case of a smooth interface, in-plane momentum conservation happens in the tunneling process, and the tunneling self-energy is given by

$$\Sigma^{\mathrm{R,A,K}}_{\mathrm{tun}} = \frac{\lambda a_{\mathrm{t}}^2 n_{\mathrm{s}}}{\hbar} \int \frac{d^3\mathrm{k}'}{(2\pi)^3} \tilde{t}^\dagger G^{\mathrm{R,A,K}}_{\mathrm{FM}} \tilde{t}\, (2\pi)^2 \delta(\mathbf{k}'_\parallel - \mathbf{p})$$
$$= \frac{\lambda a_{\mathrm{t}}^2 n_{\mathrm{s}}}{\hbar} \int \frac{d\mathrm{k}'_{\mathrm{z}}}{2\pi} \tilde{t}^\dagger G^{\mathrm{R,A,K}}_{\mathrm{FM}}(\mathbf{R}, z=0, t; \mathbf{k}'_\parallel, \mathrm{k}'_{\mathrm{z}}, \varepsilon)\tilde{t}. \tag{A17}$$

For diffusive transport in the FM, the the Keldysh components of the quasiclassical Green's functions $\tilde{g}^{\mathrm{K}}_{\uparrow,\downarrow}$ for the up and down electrons in the FM can be expanded with an isotropic and an anisotropic component (with respect to the momentum direction $\hat{\mathbf{k}}_{\uparrow,\downarrow}$). In the diffusive limit, the isotropic component will be proportional to the up and down electrochemical potential in the FM, while the anisotropic component will be determined by the spatial variation (gradient) of the isotropic component. Since the variation of the up and down electrochemical potential in the FM will be negligible [37], the anisotropic component of the quasiclassical Green's functions $\tilde{g}^{\mathrm{K}}_{\uparrow,\downarrow}$ of the FM can be neglected. So, if the quasiclassical Green's functions $\tilde{g}^{\mathrm{K}}_{\uparrow,\downarrow}$ are isotropic in $\mathbf{k}_{\uparrow,\downarrow}$ space, from Eq. (A17) we obtain that the retarded, advanced and Keldysh components of the tunneling self-energy are given by the same relation as that of Eq. (A16) with $\gamma_{\uparrow,\downarrow} = \pi\lambda t_{\uparrow,\downarrow}^2/\hbar$ and $N_{\uparrow,\downarrow}$ will be the corresponding 1D DOSs calculated with the constraint of in-plane momentum conservation.

The quantum kinetic equation in terms of the quasiclassical Green's function g^{K} of the TI surface state is obtained after performing ξ_{p} integration of Eq. (A6), which is

$$\partial_t g^{\mathrm{K}} + \frac{v_{\mathrm{F}}}{2}\{\hat{\mathbf{z}} \times \boldsymbol{\sigma} \cdot \boldsymbol{\nabla}_{\mathbf{R}}, g^{\mathrm{K}}\} + i v_{\mathrm{F}} \mathrm{p}_{\mathrm{F}}[(\hat{\mathbf{p}} \times \hat{\mathbf{z}}) \cdot \boldsymbol{\sigma}, g^{\mathrm{K}}]$$
$$= -\frac{g^{\mathrm{K}}}{\tau_{\mathrm{p}}} + \frac{\langle g^{\mathrm{K}} \rangle}{\tau_{\mathrm{p}}} + \frac{1}{2\tau_{\mathrm{p}}}\{(\hat{\mathbf{p}} \times \hat{\mathbf{z}}) \cdot \boldsymbol{\sigma}, \langle g^{\mathrm{K}} \rangle\}$$
$$- \{(\gamma_\uparrow N_\uparrow \mathrm{P}_\uparrow + \gamma_\downarrow N_\downarrow \mathrm{P}_\downarrow), g^{\mathrm{K}}\}$$
$$+ (\gamma_\uparrow N_\uparrow \mathrm{P}_\uparrow g_\uparrow + \gamma_\downarrow N_\downarrow \mathrm{P}_\downarrow g_\downarrow)$$
$$+ \frac{1}{2}\{(\hat{\mathbf{p}} \times \hat{\mathbf{z}}) \cdot \boldsymbol{\sigma}, (\gamma_\uparrow N_\uparrow \mathrm{P}_\uparrow g_\uparrow + \gamma_\downarrow N_\downarrow \mathrm{P}_\downarrow g_\downarrow)\}. \tag{A18}$$

For spin-conserving tunneling, $t_\uparrow = t_\downarrow = t_0$, and $\gamma_\uparrow = \gamma_\downarrow = \gamma$, and we obtain Eq. (1) in the main text with the identification $\mathrm{g} = g^{\mathrm{K}}$ and $\mathrm{g}_{\uparrow,\downarrow} = g_{\uparrow,\downarrow}$. However, to recover Eq. (A18) from Eq. (1), the replacement $\gamma N_\uparrow \to \gamma_\uparrow N_\uparrow$ and $\gamma N_\downarrow \to \gamma_\downarrow N_\downarrow$ should be performed.

The term $\mathbf{F} \cdot \frac{\partial f}{\partial \mathbf{p}}$ in the classical Boltzmann equation which is the term $-e\mathbf{E} \cdot \boldsymbol{\nabla}_{\mathbf{p}} G^{\mathrm{K}}$ in the quantum kinetic equation, Eq. (A6), drops out of the quantum kinetic equation, Eq. (A18), written for the Wigner transformed quasiclassical Green's function $g^{\mathrm{K}}(\mathbf{r}, \mathrm{p}_{\mathrm{F}}\hat{\mathbf{p}}, t, \varepsilon)$ after ξ_{p} integration, because of the assumption that the Fermi energy is the largest energy scale in the problem [40]. The substitution $\boldsymbol{\nabla}_{\mathbf{R}} \to \boldsymbol{\nabla}_{\mathbf{R}} + e\mathbf{E}\partial_\varepsilon$ that appears in the quantum kinetic equation for the gauge invariant Wigner-transformed Green's function $\tilde{g}^{\mathrm{K}}(\mathbf{r}, \mathbf{p}, t, \varepsilon)$ as done in Ref. [33], cancels out in the quantum kinetic equation, Eq. (A6), written for normal (not gauge invariant) Wigner transformed quasiclassical Green's function g^{K} (that we use in this work) [40], giving rise to a term proportional to $\partial_t \phi$ which is zero in case of time-independent external electrostatic potential. However, the external electrostatic potential ϕ appears in the expression for the actual nonequilibrium charge density of the electrons n_{neq} and can therefore be subsumed by defining an effective nonequilibrium charge density n, as mentioned in the main text.

In the most general case of spin-selective but spin-nonconserving tunneling, Eqs. (29)–(31) also will be modified and can be obtained by the replacement $\gamma N_\uparrow \to \gamma_\uparrow N_\uparrow$ and $\gamma N_\downarrow \to \gamma_\downarrow N_\downarrow$. Equation (29) will become

$$\begin{bmatrix} \Omega - 1 & -i\Delta_x \\ -i\Delta_x & f_2 - 1 \end{bmatrix} \begin{bmatrix} n \\ 2s_y \end{bmatrix}$$
$$= \begin{bmatrix} e^2 N \tau_{\mathrm{p}} (\gamma_\uparrow N_\uparrow \mu_\uparrow + \gamma_\downarrow N_\downarrow \mu_\downarrow) \\ e^2 N \tau_{\mathrm{p}} m_y (\gamma_\uparrow N_\uparrow \mu_\uparrow - \gamma_\downarrow N_\downarrow \mu_\downarrow) \end{bmatrix}, \tag{A19}$$

where we have $\Omega = 1 + (\gamma_\uparrow N_\uparrow + \gamma_\downarrow N_\downarrow)\tau_{\mathrm{p}} - i\omega\tau_{\mathrm{p}}$ and $\Delta_x = \mathrm{q}_x v_{\mathrm{F}} \tau_{\mathrm{p}} + i(\gamma_\uparrow N_\uparrow - \gamma_\downarrow N_\downarrow)\tau_{\mathrm{p}} m_y$. Then the modified continuity equation of the charge density on the TI surface, i.e., Eq. (30), becomes

$$d_x j_x = \gamma_\uparrow N_\uparrow (e^2 N \mu_\uparrow - n) + \gamma_\downarrow N_\downarrow (e^2 N \mu_\downarrow - n)$$
$$+ m_y (\gamma_\uparrow N_\uparrow - \gamma_\downarrow N_\downarrow) \frac{j_x}{v_{\mathrm{F}}}. \tag{A20}$$

The modified diffusion equation for the charge current density on the TI surface, i.e., Eq. (31), becomes

$$j_x = \frac{1}{(1+\xi)}\big[- v_{\mathrm{F}}^2 \tau_{\mathrm{p}} \partial_x n - v_{\mathrm{F}} \tau_{\mathrm{p}} m_y \{\gamma_\uparrow N_\uparrow (e^2 N \mu_\uparrow - n)$$
$$- \gamma_\downarrow N_\downarrow (e^2 N \mu_\downarrow - n)\}\big], \tag{A21}$$

where the new ξ will be redefined by $\xi = (\gamma_\uparrow N_\uparrow + \gamma_\downarrow N_\downarrow)\tau_{\mathrm{tr}}$. However, for $\mu_\uparrow = \mu_\downarrow = \mu_{\mathrm{c}}$, the forms of Eqs. (32) and (33) remain the same with the above-mentioned redefined ξ and a redefined η given by $\eta = (\gamma_\uparrow N_\uparrow - \gamma_\downarrow N_\downarrow)/(\gamma_\uparrow N_\uparrow + \gamma_\downarrow N_\downarrow)$.

APPENDIX B: SOLUTION OF THE TRANSPORT EQUATIONS

In this section, we provide the solution of the electrochemical potential μ on the TI surface underneath the FM for different boundary conditions corresponding to different circuit

geometries as shown in Fig. 4. From Eq. (39a), the general solution of $\mu' = (\mu - \mu_c^0)$ is given by $\mu' = A_1 e^{r_1 x} + A_2 e^{r_2 x}$, where $r_{1,2} = bm_y \pm c$, $b = \xi\eta/l_{tr}$ and $c = \sqrt{2\xi(1+\xi)}/l_{tr}$. Then from Eq. (39b), the current density j_x on the TI surface can be written as $j_x = -\sigma' c(A_1 e^{r_1 x} - A_2 e^{r_2 x})$, and the unknown constants $A_{1,2}$ are determined from the boundary conditions on j_x.

For the circuit geometries of Figs. 4(a), 4(c), and 4(e), the boundary conditions are $j_x(x=0) = 0$ and $j_x(x=L) = I/W$. Hence, μ and j_x are given by

$$\mu = \mu_c^0 - \frac{I\,\mathrm{csch}(cL)}{\sigma' cW} e^{-bm_y L}\left(\frac{e^{r_1 x} + e^{r_2 x}}{2}\right), \tag{B1a}$$

$$j_x = \frac{I\,\mathrm{csch}(cL)}{W} e^{-bm_y L}\left(\frac{e^{r_1 x} - e^{r_2 x}}{2}\right). \tag{B1b}$$

For the circuit geometries of Figs. 4(b), 4(d), and 4(f), the boundary conditions are $j_x(x=0) = I/W$ and $j_x(x=L) = 0$. Hence, μ and j_x are given by

$$\mu = \mu_c^0 + \frac{I\,\mathrm{csch}(cL)}{\sigma' cW}\left(\frac{e^{r_1 x - cL} + e^{r_2 x + cL}}{2}\right), \tag{B2a}$$

$$j_x = -\frac{I\,\mathrm{csch}(cL)}{W}\left(\frac{e^{r_1 x - cL} - e^{r_2 x + cL}}{2}\right). \tag{B2b}$$

For the circuit geometries of Figs. 4(g) and 4(h), the boundary conditions are $j_x(x=0) = j_x(x=L) = I/W$. Hence, μ and j_x are given by

$$\mu = \mu_c^0 - \frac{I}{\sigma' cW}\left[\frac{(1-e^{r_2 L})e^{r_1 x} + (1-e^{r_1 L})e^{r_2 x}}{(e^{r_1 L} - e^{r_2 L})}\right], \tag{B3a}$$

$$j_x = \frac{I}{W}\left[\frac{(1-e^{r_2 L})e^{r_1 x} - (1-e^{r_1 L})e^{r_2 x}}{(e^{r_1 L} - e^{r_2 L})}\right]. \tag{B3b}$$

Equations (40), (41), and (42) are obtained from Eqs. (B1a), (B2a), and (B3a), respectively.

The tunneling current density j_{tun} flowing from the FM to the TI surface through the interface is given by the right-hand side of the modified continuity equation for transport on the TI surface, i.e., Eq. (32). So, we have

$$j_{tun} = \frac{2\xi\sigma}{l_{tr}^2}(\mu_c^0 - \mu) + \frac{\xi\eta m_y}{l_{tr}} j_x, \tag{B4}$$

and, the modified continuity equation for transport on the TI surface now can be written as

$$d_x j_x = j_{tun}. \tag{B5}$$

After integrating the above equation, i.e., Eq. (B5), from 0 to L, and using the fat that $\int_0^L dx\, d_x j_x = j_x(L) - j_x(0)$, we obtain the total tunneling current density j_{tun}^{tot} to be

$$j_{tun}^{tot} = \int_0^L dx\; j_{tun} = j_x(L) - j_x(0). \tag{B6}$$

The above equation, i.e., Eq. (B6), implies current conservation. In all the cases considered above, using Eqs. (B1)–(B3) it is straightforward to check that the current conservation holds.

[1] M. Z. Hasan and C. L. Kane, Rev. Mod. Phys. **82**, 3045 (2010).

[2] C. H. Li, O. M. J. van't Erve, J. T. Robinson, Y. Liu, L. Li, and B. T. Jonker, Nat. Nanotechnology **9**, 218 (2014).

[3] J. Tang, L.-T. Chang, X. Kou, K. Murata, E. S. Choi, M. Lang, Y. Fan, Y. Jiang, M. Montazeri, W. Jiang, Y. Wang, L. He, and K. L. Wang, Nano Lett. **14**, 5423 (2014).

[4] A. Dankert, J. Geurs, M. V. Kamalakar, S. Charpentier, and S. P. Dash, Nano Lett. **15**, 7976 (2015).

[5] L. Liu, A. Richardella, I. Garate, Y. Zhu, N. Samarth, and C.-T. Chen, Phys. Rev. B **91**, 235437 (2015).

[6] J. S. Lee, A. Richardella, D. R. Hickey, K. A. Mkhoyan, and N. Samarth, Phys. Rev. B **92**, 155312 (2015).

[7] E. K. de Vries, A. M. Kamerbeek, N. Koirala, M. Brahlek, M. Salehi, S. Oh, B. J. van Wees, and T. Banerjee, Phys. Rev. B **92**, 201102(R) (2015).

[8] F. Yang, S. Ghatak, A. A. Taskin, K. Segawa, Y. Ando, M. Shiraishi, Y. Kanai, K. Matsumoto, A. Rosch, and Y. Ando, Phys. Rev. B **94**, 075304 (2016).

[9] A. Dankert, P. Bhaskar, D. Khokhriakov, I. H. Rodrigues, B. Karpiak, M. V. Kamalakar, S. Charpentier, I. Garate, and S. P. Dash, Phys. Rev. B **97**, 125414 (2018).

[10] C. H. Li, O. M. van't Erve, S. Rajput, L. Li, and B. T. Jonker, Nat. Commun. **7**, 13518 (2016).

[11] C. H. Li, O. M. J. van't Erve, Y. Y. Li, L. Li, and B. T. Jonker, Sci. Rep. **6**, 29533 (2016).

[12] C. H. Li, O. M. J. van't Erve, C. Yan, L. Li, and B. T. Jonker, Sci. Rep. **8**, 10265 (2018).

[13] J. Tian, I. Miotkowski, S. Hong, and Y. P. Chen, Sci. Rep. **5**, 14293 (2015).

[14] Y. Ando, T. Hamasaki, T. Kurokawa, K. Ichiba, F. Yang, M. Novak, S. Sasaki, K. Segawa, Y. Ando, and M. Shiraishi, Nano Lett. **14**, 6226 (2014).

[15] S. Hong, V. Diep, S. Datta, and Y. P. Chen, Phys. Rev. B **86**, 085131 (2012).

[16] T. Yokoyama and Y. Tserkovnyak, Phys. Rev. B **89**, 035408 (2014).

[17] P. Li and I. Appelbaum, Phys. Rev. B **93**, 220404(R) (2016).

[18] S. Hong, S. Sayed, and S. Datta, Sci. Rep. **6**, 20325 (2016).

[19] S. Sayed, S. Hong, and S. Datta, Sci. Rep. **6**, 35658 (2016).

[20] S. Sayed, S. Hong, E. E. Marinero, and S. Datta, IEEE Electron Device Lett. **38**, 1665 (2017).

[21] U. Roy, R. Dey, T. Pramanik, B. Ghosh, L. F. Register, and S. K. Banerjee, J. Appl. Phys. **117**, 163906 (2015).

[22] M. Buttiker, IBM J. Res. Dev. **32**, 317 (1988).

[23] A. A. Burkov and D. G. Hawthorn, Phys. Rev. Lett. **105**, 066802 (2010).

[24] P. Schwab, R. Raimondi, and C. Gorini, Europhys. Lett. **93**, 67004 (2011).

[25] K. Taguchi, T. Yokoyama, and Y. Tanaka, Phys. Rev. B **89**, 085407 (2014).

[26] R. Dey, A. Roy, T. Pramanik, A. Rai, S. Heon Shin, S. Majumder, L. F. Register, and S. K. Banerjee, Appl. Phys. Lett. **110**, 122403 (2017).
[27] M. Götte, T. Paananen, G. Reiss, and T. Dahm, Phys. Rev. Appl. **2**, 054010 (2014).
[28] Y. G. Semenov, X. Duan, X.-L. Li, and K. W. Kim, J. Phys. Chem. Solids **128**, 196 (2019).
[29] J. Tian, I. Childres, H. Cao, T. Shen, I. Miotkowski, and Y. P. Chen, Solid State Commun. **191**, 1 (2014).
[30] S. Majumder, S. Guchhait, R. Dey, L. Register, and S. K. Banerjee, IEEE Trans. Nanotech. **15**, 671 (2016).
[31] M. Zhang, X. Wang, S. Zhang, Y. Gao, Z. Yu, X. Zhang, M. Gao, F. Song, J. Du, X. Wang, L. He, Y. Xu, and R. Zhang, IEEE Electron Device Lett. **37**, 1231 (2016).
[32] E. I. Rashba, Phys. Rev. B **68**, 241315(R) (2003).
[33] E. G. Mishchenko, A. V. Shytov, and B. I. Halperin, Phys. Rev. Lett. **93**, 226602 (2004).
[34] R. Dey, L. F. Register, and S. K. Banerjee, Phys. Rev. B **97**, 144417 (2018).
[35] X. Liu and J. Sinova, Phys. Rev. Lett. **111**, 166801 (2013).
[36] R. Dey, N. Prasad, L. F. Register, and S. K. Banerjee, Phys. Rev. B **97**, 174406 (2018).
[37] Considering transport within the FM contact,it was shown [16] that the charge electrochemical potential $\mu_c(x)$ in the FM will be some constant (μ_c^0) plus a variation ($\mu_c^1(x)$) along the length of the contact,i.e.,$\mu_c = \mu_c^0 + \mu_c^1(x)$,where $\mu_c^1(x)$ will be proportional r,the ratio of the conductivity of the TI surface to that of the FM. Similarly,it can be shown that the spin electrochemical potential $\mu_s(x)$ in the FM will be proportional to r. However,since typically r is a small quantity,$\mu_c^1(x)$ and $\mu_s(x)$ can be neglected with respect to μ_c^0,and μ_c can be taken as constant within the FM.
[38] The Hamiltonian in our work is different from the one used previously [36] and can be obtained from the later after changing $\hat{\mathbf{z}} \rightarrow -\hat{\mathbf{z}}$. So,all the results of our previous work can be used in this work after making the substitution $\hat{\mathbf{z}} \rightarrow -\hat{\mathbf{z}}$. To obtain Eq. (45) of this work from Eq. (13) of our previous work [36],we have made the substitution $\hat{\mathbf{z}} \rightarrow -\hat{\mathbf{z}}$ in Eq. (13) of our previous work.
[39] J. Tian, S. Hong, I. Miotkowski, S. Datta, and Y. P. Chen, Sci. Adv. **3**, e1602531 (2017).
[40] C. Gorini, Quasiclassical methods for spin-charge coupled dynamics in low-dimensional systems, Doctoral thesis, Universität Augsburg, 2010.